

| | |
|-------------------------------|---|
| Grant Agreement no.: | 824066 |
| Project acronym: | E-MAGIC |
| Project title: | European Magnesium Interactive Battery Community |
| Type of Action: | Research and Innovation Action (RIA) |
| Topic: | FETPROACTIVE-01-2018 - Disruptive micro-energy and storage technologies |
| Start date of project: | 01.01.2019 |
| Duration: | 48 months |
| Project Coordinator: | Fundación CIDETEC (ES) |

Deliverable (Type¹: R)
Report on basic electrolyte based on glymes, MgCl₂, Mg(TFSI)₂
(D 2.3 / participation portal: D04)

| | |
|---------------------------------------|---|
| Author (partner): | Ayan Mukherjee (BIU) |
| Other authors: | Doron Aurbach (BIU), Malachi Noked (BIU). |
| Work package No. Title: | WP2 Anode and Electrolyte System |
| Work package leader (partner): | BIU |
| Date released by WP leader: | 06/06/2020 |
| Date released by Coordinator: | 14/06/2020 |

| Dissemination level | |
|---------------------|---|
| PU | Public X |
| CO | Confidential, only for members of the consortium (including the Commission Service) |
| CI | Classified, information as referred to in Commission Decision 2001/844/EC. |

¹**R:** Document, report (excluding the periodic and final reports).

DEM: Demonstrator, pilot, prototype, plan designs.

DEC: Websites, patents filing, press & media actions, videos, etc.

OTHER: Software, technical diagram, etc.



Revisions

| Version | Date | Changed by | Comments |
|---------|------------|---------------|--|
| V1 | 06/06/2020 | A. Mukherjee | Version submitted to coordinator by BIU |
| V1b | 09/06/2020 | L. Colmenares | Intensive editing and quality check |
| V2 | 13/06/2020 | A. Mukherjee | Revised draft |
| V2 | 14/06/2020 | L. Colmenares | New draft accepted and shared with rest of partners. |
| final | 22/06/2020 | L. Colmenares | Draft accepted by entire consortium. Quality check done. |

Distribution restricted to the E-MAGIC consortium.



Table of Content

| | |
|--|----|
| Table of Content..... | 3 |
| 1 Introduction | 4 |
| 2. How solution chemistry affects the electrochemical behavior of cathodes for Mg batteries, a classical electro-analytical study. | 4 |
| 2.1. Qualitative analysis of the slow sweep rate cyclic voltammetry:..... | 4 |
| 2.2. Rate determining steps of the voltammetric response: semi-infinite diffusion versus ion accumulation in the solid host..... | 6 |
| 2.3. Solid state diffusion of Mg ions in the Chevrel phase – choosing the right mathematical model:..... | 9 |
| 2.4. The effect of the electrolyte solutions on the interfacial charge transfer across the electrodes interface: | 10 |
| 2.5. Conclusions: | 12 |
| 3. TFSI containing electrolyte solution effects on high voltage cathode electrochemical activity in rechargeable magnesium batteries | 12 |
| 4. Solvent effects on the reversible intercalation of Mg ions into V ₂ O ₅ electrodes..... | 16 |
| 4.1. Non- aqueous magnesium electrochemistry – the effect of the presence of DME in ACN solutions on the electrochemical performances of V ₂ O ₅ electrodes..... | 16 |
| 4.2. Solutions structure – solvation effects | 20 |
| 4.3. Surface analysis | 23 |
| 4.4. Conclusions: | 25 |
| 5. The role of surface adsorbed Cl ⁻ complexes in rechargeable magnesium batteries | 25 |
| 5.1. Conclusions | 35 |
| 6. Final highlights | 36 |
| 7. Reference..... | 36 |



1 Introduction

The hurdles in Mg intercalation processes stems from both kinetic and thermodynamic limitations, as well as surface/interfacial complications. The Mg ion bivalency and its small ionic radius leads to sluggish solid-state diffusion and difficulty in maintaining local electroneutrality within the crystalline hosts during equilibrium [1]. Up to date only Chevrel phase based (CP) cathodes exhibit reversible Mg ions intercalation with reasonable kinetics. Despite CP's reversible Mg insertion, its relatively low intercalation potential and low specific capacity renders it insufficient for practical systems. The lack of any other high voltage/capacity host material for Mg ions hampers the development of practical RMBs.

Rational development of novel cathode materials requires several basic understandings, among them thorough knowledge of the complicated mechanism of Mg intercalation and its relation to the electrolytic solution's nature. Some in-depth studies have already revealed that the chemical, electrochemical, interfacial and the physical processes associated with the intercalation reactions are, sometimes, much more complicated than the ion's solid-state diffusion and phase changes alone. The ability of ions, atoms, or even molecules to reversibly insert into crystalline materials is frequently perceived to be dependent only on the aptitude of the inserted ions to occupy available sites in the crystalline host material and the associated solid-state chemical changes. In reality, however, interfacial interactions prove to be way more complicated and key factors to the material's function as insertion compound.

It had already been established that some electrochemical intercalation reactions, especially in the case of Mg ions, are strongly electrolyte solution dependent. For example, α - V_2O_5 was found to be inactive in MgTFSI₂/AN solution, while electrochemically active in Mg(ClO₄)₂/AN [2]. In addition, had been demonstrated that the electroanalytical behavior of Mg intercalation processes into CP is different in 0.25M AlCl₃ + 0.5M PhMgCl/THF (APC) then in 0.25M MgTFSI₂+ 0.5M MgCl₂/DME (ICD) [3]. In another words, Mg intercalation processes into crystalline hosts is, at least in some cases, is strongly influenced by the electrolyte solution or by a synergy between the cathode and specific species in the electrolyte solution. The reason for these effects lies in the complex, sequential chemical and electrochemical reactions steps encompassing the complete intercalation reaction mechanism. These can be charge transfer across two different interphases, infinite solid-state diffusion, semi-infinite solid-state diffusion, accumulation and specific surface and interfacial reactions and interactions. Each component in the electrolyte solution may have substantial effect on one or several of these steps, in kinetic or thermodynamic terms.

Most of the electrolyte solutions explored for rechargeable Mg system comprise Cl-based ions [4–8] These provide several functions, among them, lowering the overpotential for deposition, enhancing magnesium deposition kinetics [9], expanding the electrochemical stability window and improving the metal deposition Faradaic reversibility.

In the follow, the deliverable D2.2 is presented as an overview of the finding and highlights from different systematic studies performed recently at BIU in frame of E-MAGIC project. Part of those outcomes has been recently published in references [2] and [3] and other ones are in review process at the time this deliverable is submitted. In that sense, ***this deliverable will be public as soon as the last submitted manuscript regarding the topic presented hereafter is accepted for publication.***

2. How solution chemistry affects the electrochemical behavior of cathodes for Mg batteries, a classical electro-analytical study.

2.1. Qualitative analysis of the slow sweep rate cyclic voltammetry:

The aim of the work described in this section was to determine qualitatively, how the electrolyte solutions nature (the electroactive complexes and the solvents) influences the kinetics and the thermodynamics of the intercalation process into the CP electrodes selected for this study. It is important to note that the fact that the



Chevrel phase (CP) material used herein include a few percent of copper is very important. It provides an extra red-ox activity which enable to emphasize clearly solutions effects, as described later herein.

For this study, high resolution slow scan rates CV (SSCV) was proven as a very useful electro-analytical tool. **Figure 2.1** presents SSCV responses of the CP electrodes in APC and ICD at three different scan rates. The voltammograms in **Figure 2.1** reflect several cathodic and anodic processes. The basic electrochemical responses of $\text{Cu}_x\text{Mo}_6\text{S}_8$ electrodes and the structural changes they reflect are well known.

In brief, the structure of these materials includes octahedral clusters of Mo_6 confined in cubes of S_8 . Between each 2 Mo_6S_8 cell unites there are 2 sets of 6 intercalation sites each (denotes as inner and outer rings of sites) that can accommodate 2 Mg ions (one per ring of sites). The initial response of these materials includes indeed insertion of two Mg ions per unit cell to form $\text{Mg}_2\text{Mo}_6\text{S}_8$. The first insertion process of Mg ions into the outer sites is lousy (**Figure 2.1** peak a). This is well reflected by the broad corresponding anodic peak b in the range 1.4-1.6 V. At room temperature a fraction of Mg ions remains trapped in the outer rings of intercalation sites and thereby at steady state the first reversible process (peak a) involves only partial insertion of Mg ions. In turn, the second process (**Fig. 1** peak c) involves a fully reversible insertion of one Mg ion per unit cell, accommodated by the inner intercalation sites. Anodic peak d reflects the fast de-intercalation of the second Mg ion. When the CP includes any fraction of residual Cu, Mg ions insertion involves a very complex reversible extrusion of atomic clusters of Cu reflected herein in the small cathodic peaks e, f to which the small anodic peaks g, h, i belong. Hence, very the minor amount of Cu detected by ICP is clearly reflected by the voltammetric response of this material. Due to the small amounts of Cu in the CP studied herein, features e – i in charts 1a,b are rather small.

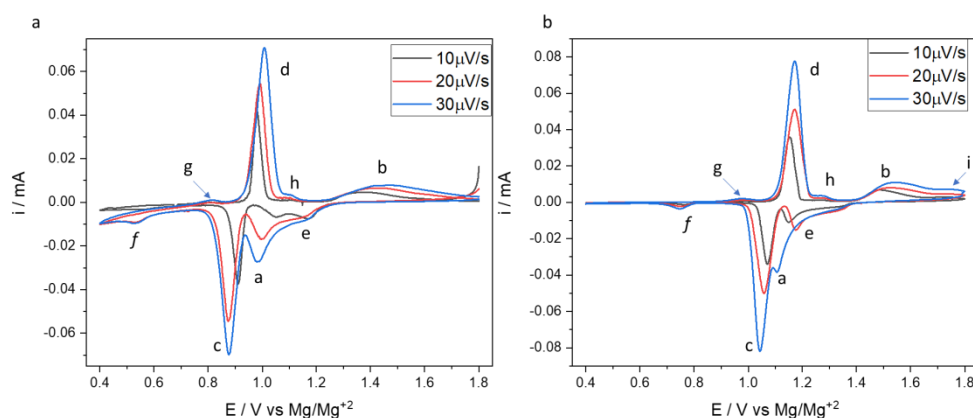


Figure 2.1: Slow scan rate cyclic voltammograms for $\text{Cu}_{0.09}\text{Mo}_6\text{S}_8$ electrodes in (a) $\text{MgTFSI}_2+\text{MgCl}_2/\text{DME}$ (ICD) and (b) APC electrolyte solutions.

It works intentionally herein with this material in order to emphasize the sensitivity of the electro-analysis that was applied. The CVs measured with the two solutions yielded basically similar electrochemical responses, but with a significant potential shift. The cathodic peaks in the voltammograms related to APC solutions appears at potentials 160 mV higher compared to those measured with ICD solutions: The formal potential of process c is around 1.11 and 0.945 V vs Mg in APC and ICD solutions respectively. These potential differences were consistent throughout all the study.

Based on extensive experience with Mg non-aqueous electrochemistry we know that an important factor which determines the over-potential developed at any electrode/solution interface in reactive Mg based electrolyte solutions relates to solvation/de-solvation interactions of Mg ions. The situation with ethereal Mg salt solutions are complicated than most of other solutions containing metallic based electrolytes (e.g. Li, Na, K, Fe). There are, apparently, several mechanisms that lead to this complexity: in many cases (especially ethereal solutions) magnesium electrolyte solutions contain complex-cations, frequently in equilibrium with other solution species. This in contrast to simple solvated ions or/and ion-pairs as in most of monovalent ions solutions.



Surface phenomena at the metallic Mg RE- solution interface also play an important, not fully predictable role. It is important to note that there were consistent differences in the coulombic efficiencies associated with cycling CP electrodes in the two solutions. While in APC the coulombic efficiency was very close to 100%, in ICD solutions it reached around 85-90%.

In light of previous studies of CP electrodes the lower faradaic efficiency obtained in ICD solutions does not reflect mismatch in charges related to the intercalation/de-intercalation processes. It rather reflects irreversible parasitic reactions associated with TFSI, as had been reported before. It had been reported that TFSI, despite being envisaged as very stable species, does irreversibly reacts electrochemically even under mild conditions. Thereby, we believe that the intrinsic coulombic efficiency associated with the insertion and de-insertion of Mg (and Cu) with CP electrodes in $\text{MgTFSI}_2 + \text{MgCl}_2 / \text{DME}$ is very high.

The shape of the CVs which reflect the electrochemical response related to Mg intercalation/de-intercalation (features a – d) and Mg \leftarrow \rightarrow Cu displacements (features e – i) is strongly affected by the solutions' nature. The peaks' separation in the CVs related to the ICD solutions is sharper (e.g. a better separation among the cathodic peaks a, c and e). This indicates that the slower (first) Mg intercalation process and the first Mg-Cu displacement stage are more thermodynamically favorable in ICD than in APC solutions. Furthermore, the electrochemical activity of these processes seems to be higher in ICD than that in APC solutions, as reflected at the higher scan rates ($>20 \mu\text{V/s}$). Interestingly, at scan rate of $30 \mu\text{V/s}$, the voltammetry of these cathodes in APC solutions resembles that for pure, Cu-free Mo_6S_8 , electrodes except for the small reduction peak f and oxidation peak h which remain indicative of the $\text{Cu}_x\text{Mo}_6\text{S}_8$ phase. These results suggest that the electrochemical activity of these CP electrodes related to the Mg-Cu displacement, is kinetically slower in APC than in ICD solutions.

All these results point towards significant influence of the solution nature on the thermodynamic and kinetic properties of both electrochemical processes (i.e. Mg ions intercalation into $\text{Cu}_x\text{Mo}_6\text{S}_8$ and Mg - Cu displacements in the CP host material).

Additional interesting feature is seen in **Figure 2.1**. The two main redox peaks potentials are scan-rate dependent in the two solutions, although to different extent. At such low scanning rates it cannot be related to the effect of an IR drop (with an influence of the specific solutions' conductivity on it). In both cases reduction peaks a and c shift to lower potentials as the potential scanning rate increases from 10 to $30 \mu\text{V/s}$. In ICD solutions a shift of 39 mV in peak c is seen by increasing the scanning rate from 10 to $30 \mu\text{V/s}$, whereas in APC solutions the shift is 11 mV, more than 3 times lower. Such response indicates that the intercalation process associated with the most pronounced Mg intercalation process (reflected by peak c) reaches equilibrium faster in APC than in ICD solutions.

2.2. Rate determining steps of the voltammetric response: semi-infinite diffusion versus ion accumulation in the solid host.

Cyclic voltammetry at wide potential scanning rates is a very powerful analytical technique. In fact, for many electrochemically active materials, CV may be much more sensitive and accurate than spectroscopy, microscopy and XRD for detecting structural and chemical changes. Quantitative and qualitative information can be deduced by comprehensive interpretation of voltammograms, especially when using appropriate mathematical models.

Electrochemical intercalation reactions are distinguished from classical electrochemical reactions involving redox couples in solution phase or at interfaces. In classical electrochemical reactions two limiting factors may be usually encountered: (i) charge transfer across the interface and (ii) electroactive species diffusion in the solution. With intercalation reactions there can be at least three limiting factors and they involve at least two iii) bulk redox reactions and solid state diffusion within the host material. Under many circumstances, the significance of these processes as *rate determining steps* may change with increasing potential scanning-rate in the following order: charge transfer across the interface, infinite solid-state diffusion, semi-infinite solid-state diffusion, and accumulation of intercalated species within the host bulk. These limiting factors, or rate determining steps (RDS), can be identified and quantified using cyclic voltammetry at different scan rates.



In the case of solid-state diffusion limited behavior with semi-infinite boundary conditions the peak current (I_p) vs. scan rate (ν) function may be expressed by the Randles-Sevcik equation:

$$I_p = 2.69 * 10^5 n^{1.5} A \sqrt{D\nu} \Delta C \quad (\text{Eq. 1})$$

Where n is the number of the electrons involve in the specific reaction, A is the electrode real surface area obtained from BET measurements, D is the solid-state diffusion coefficient, and ΔC is the change in the Mg ions concentration inside the host material during the specific stage.

It is important to note that **Equation 1** was developed for Nernstian redox reactions across single interfaces with a constant electroactive bulk concentration. In addition, this equation is correct only for reversible redox reaction. Also, the theory relates to systems which diffusion coefficient is constant, potential invariant. This may not be the case for solid-state diffusion of many intercalation electrodes. However, Randles-Sevcik equation may be adequate as a first approximation for the situation around the peak's potential, because a very small amount of charge is injected around the peak potential, compared with the entire process.

In contrast to semi-infinite diffusion limited process, accumulation limited process can be characterized by the following relationship, which related to Langmuir type isotherm:

$$I_p = 9.39 * 10^5 * \nu l A \Delta C \quad (\text{Eq. 2})$$

Where l is the electrode thickness.

The analysis described below relates to the two consecutive Mg ions insertion processes denote in **Figure 2.1** as peaks a and c. **Figure 2.2** shows the peak current as a function of the scanning rate for the 2 magnesium intercalation processes in the two solutions (i.e. APC and MgTFSI₂+MgCl₂/DME).

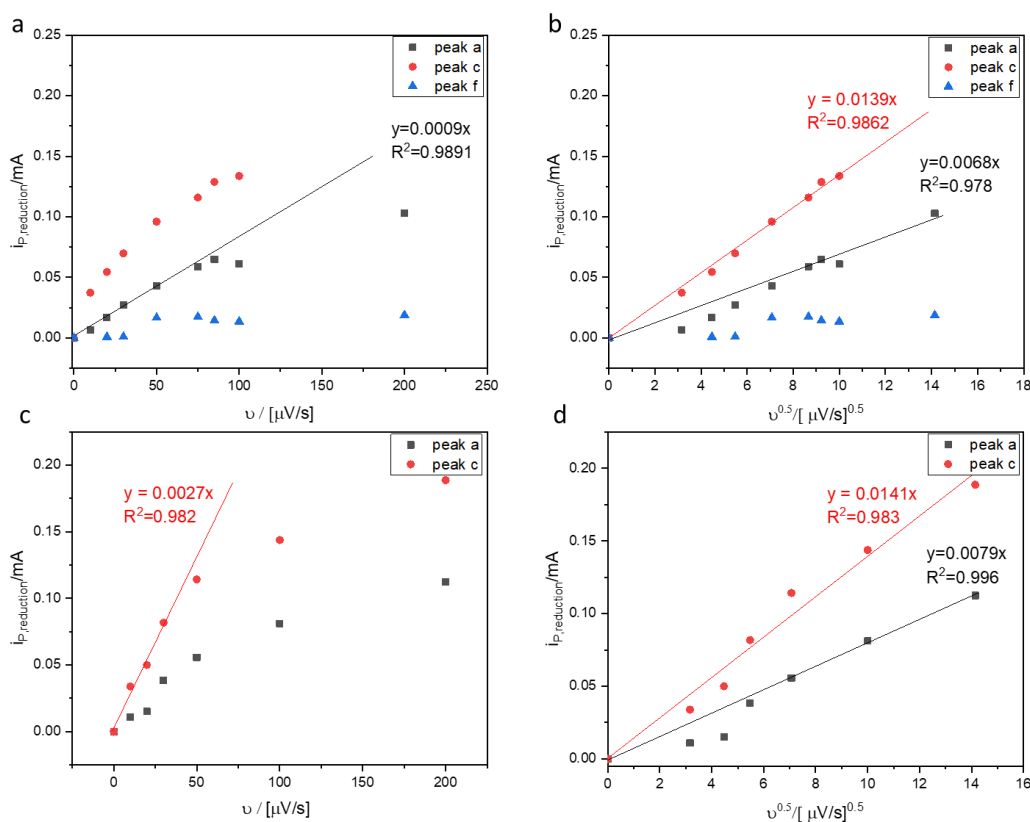


Figure 2.2: the dependence of the reduction peaks heights on the potential scan rates for a and c process in (a,b) MgTFSI₂+MgCl₂/DME and (c,d) APC electrolyte solutions.



Analyzing the peak current vs. scanning rate curves for ICD solutions reveal interesting voltammetric behavior. The first intercalation process indexed as *peak a* exhibits two scanning rate dependences limiting behaviors. At slow scan rates (10-50 $\mu\text{V/s}$) the peak current is linearly proportional to v . Hence, at the slow scan rates the intercalation process associated with *peak a* is accumulation controlled. At higher scan rates the peak current fits better to \sqrt{v} , indicating that the process is under solid-state diffusion control.

On the other hand, the second Mg intercalation process, associated with *peak c*, shows that the peak current fits well linear correlation with \sqrt{v} rather than v , even at the slowest scan rates (included (0,0) point). This indicates that the magnesium insertion reaction related to *peak c* (actually the main Mg intercalation process), is mainly controlled by semi-infinite solid-state diffusion. Interestingly, even at the slowest scan rate in this study, 10 $\mu\text{V/s}$, this current/voltage response of this process does not conform to accumulation-controlled reaction (does not reach quasi-equilibrium).

Another interesting insight can be learned from *peak f*, which is associated directly to concomitant Mg intercalation and copper extrusion (i.e. Mg – Cu displacement). *Peak f* shows no relation to any typical limiting behavior discussed above. This indicates that this conversion step exhibits different limiting behavior during CV, associated with different reaction dynamics, rather than simple charge transfer across the interface, solid-state diffusion or accumulation. It might constitute mixed kinetics associated with several internal, solid-state, and interfacial processes.

The electrochemical intercalation reactions in APC exhibit also two limiting cases.

The magnesium insertion reaction related to *peak a* (the first Mg intercalation process) exhibits a single limiting behavior, in contrast to the situation in the ICD solutions. The peak current shows better linear relations to \sqrt{v} all over the tested scan rates. However, there are two linear regions in the I_p vs. \sqrt{v} curve (10-20 and 30-200 $\mu\text{V/s}$). The results indicate that the intercalation process associated with *peak a* may become accumulation-controlled only at the extreme low scan rates.

The second magnesium intercalation process, *peak c*, exhibits two limiting behaviors depending on the scan rates. At slow scan rates (10-30 $\mu\text{V/s}$), the peak current is linearly proportional to v . Hence, at slow scan rates the intercalation reaction is accumulation-controlled. At higher scan rates, the peak current is linearly proportional to \sqrt{v} , indicating that the process is under solid-state diffusion control.

It is very important to note that any linear fitting in these cases must obtain curve that goes to 0 at the origin, namely, 0,0 point.

As an intermediate conclusion, the data analysis shows that magnesium intercalation kinetics into Cu-containing Chevrel phase electrodes is solution dependent. It comes that the rate determining step of process *c* has a quasi-equilibrium character at low scan rates in APC. While, in $\text{MgTFSI}_2 + \text{MgCl}_2 / \text{DME}$ electrolyte solution (ICD), the same process is semi-infinite diffusion limited even at the slowest scan rates.

The process associated with *peak a* (associated mostly with the first magnesium ions intercalation, first stage, and the beginning of copper ions displacement), yields opposite trend. At slow scan rates the electrochemical process in ICD solutions exhibits quasi-equilibrium characteristics, while in APC solutions it is semi-infinite solid-state diffusion controlled, even at the slowest scan rates.

Table 2.1: Summary of the processes limiting factors obtained from I_p vs. v in slow-scan rates with $\text{Cu}_{0.09}\text{Mo}_6\text{S}_8$ in APC and ICD solutions.

| Peak (process) | Slow scan rates | | Fast scan rate | |
|--|-------------------------|-------------------------|----------------------|----------------------|
| | <i>a</i> | <i>c</i> | <i>a</i> | <i>c</i> |
| APC | Diffusion controlled | Accumulation controlled | Diffusion controlled | Diffusion controlled |
| $\text{MgTFSI}_2 + \text{MgCl}_2 / \text{DME}$ | Accumulation controlled | Diffusion controlled | Diffusion controlled | Diffusion controlled |



2.3. Solid state diffusion of Mg ions in the Chevrel phase – choosing the right mathematical model:

In order to further shed light on the different reaction dynamics of these systems, it has carried out combined CV and GITT experiments. These techniques may yield comparative, indirect, information regarding the electroactive species undergoing insertion into the solid host (*i.e.* “naked” Mg ions or complex ions). Such data will be used to study the nature of the electrolyte solution influence, if there is any, on the solid-state diffusion of the electroactive ions inside the host material.

The calculations of the diffusion coefficients from the CV measurements were done using two different models: Nernstian reversible and irreversible reactions. As mentioned above, these two models were developed for redox process occurring on a single interface while the bulk redox concentrations remain constant. Hence, the quantitative analysis using these models can be considered here only as a first approximation. The calculated diffusion coefficients were compared with the diffusion coefficient calculated from GITT. GITT is especially adequate for the study of solid-state electrochemical processes, as it was developed by solving two differential equations for the second Fick's law with specific boundary conditions of the transient currents. Systematic GITT measurements allow to develop the diffusion coefficient as a function of potential and the content of Mg ions in the host along the intercalation process.

- ✓ For the reversible Nernstian model Equation 1 was used.
- ✓ For the irreversible redox system, the diffusion coefficients were calculated using the following equation:

$$i_p = 2.99 \times 10^5 \alpha^{0.5} A \Delta c D^{0.5} \nu^{0.5} \quad (\text{Eq. 3})$$

Where α is the transfer coefficient (choose to be 0.5).

The difference in the $i_p(\nu)$ functions for these two models is due to the different boundary conditions used to solve the Nernst-Fick, time-dependent equations. Hence, $i(t)$ and $i_p(\nu)$ functions are different.

For calculating the diffusion coefficients from the GITT response the Equation 4 was used:

$$D = \frac{4}{\pi \tau} \left(\frac{m_b V_M}{M w_b S} \right)^2 \left(\frac{\Delta E_S}{\Delta E_t} \right)^2 \quad (\text{Eq. 4})$$

Where τ represent the duration of the applied current stage, m_b is the electrode active mass, V_M is the molar volume of the electrode material, $M w_b$ is the electrode's active material molar mass, S is the electrode's surface area (calculated from BET measurements), ΔE_S is the voltage change during the OCV period, and ΔE_t is the voltage change during the galvanostatic polarization stage.

The tabulated results are presented in **Table 2.2**.

Table 2.2: solid state diffusion coefficients in cm^2/s of Mg ions in Mo_6S_8 calculated from CV and GITT measurements:

| | Peak | Nernstian reversible | Irreversible | GITT |
|-------------------|------|----------------------|---------------------|---------------------|
| MgTFSI2+MgCl2/DME | a | 6×10^{-16} | 8×10^{-15} | 2×10^{-16} |
| | c | 2×10^{-15} | 2×10^{-14} | 3×10^{-15} |
| APC | a | 8×10^{-16} | 1×10^{-14} | 8×10^{-16} |
| | c | 2×10^{-15} | 2×10^{-14} | 1×10^{-15} |

The data indicate that the solid-state diffusion coefficients are independent on the electrolyte solution identity. This conclusion, while not unexpected, has important implications. The Mg species existing in the two solutions are very different, as well as their solvation shells. For instance, DME is well known to yield very stable Mg-3DME^{++} solvates. These can be expected to intercalate as whole entities. Such co-intercalation eliminates the energy penalty upon disintegration of the solvated ions on the way to release naked Mg^{+2} ions and screen the high charge density of the naked ions within the host's crystal. The results point out that even with different electroactive



species in the solutions ($[5\text{DME}\cdot\text{Mg}_3\text{Cl}_4]^{2+}$ and $[6\text{THF}\cdot\text{Mg}_2\text{Cl}_3]^+$ for $\text{MgTFSI}_2+\text{MgCl}_2/\text{DME}$ and for APC solutions, respectively) the ions moving inside the host material diffuse at solutions independent rates. This indicates that the same (probably naked Mg ions) are inserted to the $\text{Cu}_{0.09}\text{Mo}_6\text{S}_8$.

It is expected that very different ionic species will show considerably different diffusion coefficients. It is important to note that the exact value of the diffusion coefficient is meaningless in such calculation, but the order of magnitude is important. The calculations anyway provide approximated average values. Nevertheless, the comparative studies are valuable, since the question is well defined: solution involvement/influence. Also, the measurements and related analyses were carried out in a quite similar manner.

In addition, the above electroanalytical studies used GITT and the calculations of D derived from them as an important indicator, how to use in parallel the CV measurements for calculating the diffusion coefficient. The CV data can be used through calculations based on the Nernstian reversible reactions model or the model suitable for irreversible reactions. It became clear that for the present study, using a relatively simple model, the former one, was relevant for calculating D from the CV data.

2.4. The effect of the electrolyte solutions on the interfacial charge transfer across the electrodes interface:

It has been demonstrated above that $\text{Cu}_{0.09}\text{Mo}_6\text{S}_8$ electrodes exhibit the same bulk-associated electrochemical characteristics in the different solutions (*i.e.*, the same limiting voltammetric behavior and the same diffusion coefficients).

Yet, there are marked differences in the CV responses that raise the assumption that there are still differences in the electrochemical reactions in the two solutions. Moreover, it had been shown in numerous studies that the electrochemistry of magnesium is particularly sensitive to solutions structure.

It hypothesizes, thus, that the different electroactive species in the solutions have substantial impact on the charge transfer processes across the electrode/solution interface. This dissimilarity should originate from the different activation energies required to strip Mg ions from the different complexes, $[5\text{DME}\cdot\text{Mg}_3\text{Cl}_4]^{2+}$ and $[6\text{THF}\cdot\text{Mg}_2\text{Cl}_3]^+$ for $\text{MgTFSI}_2+\text{MgCl}_2/\text{DME}$ and APC, respectively. Another possible impact may be related to a difference in the surface chemistry of the CP cathodes in contact with the different electrolyte solutions. For instance, the processes associated with **peaks a** and **f** involve the extrusion of neutral Cu atoms to the host's surface, as was explained above. In such instance, strong interactions of Cu with the solutions may lead to differences in the interfacial reactions.

In order to test the hypothesis, it calculated the heterogeneous rate constants for Mg ion charge transfer across the electrodes interfaces in both electrolyte solutions.

For that it used the model for quasi-reversible redox systems. Under this framework, the dimensionless rate parameter ψ must be determined. The heterogeneous rate constant can be determined from the definition of this dimensionless rate parameter, as depicted in the following Equation 5.

$$\psi = \frac{\left(\frac{D_O}{D_R}\right)^{\alpha/2} K_S}{[D_R \pi \nu \left(\frac{nF}{RT}\right)]^{0.5}} \quad (\text{Eq. 5})$$

Where D_O and D_R are the diffusion coefficients for the de-intercalation and intercalation processes. D_O and D_R were assumed to be equal and were taken from the GITT measurements ($D=10^{-15} \text{ cm}^2/\text{s}$). F is faraday constant, R is the universal gas constant, T is the temperature, and K_S is the heterogeneous rate constant.

In order to find the linear function $\psi\left(\frac{1}{\sqrt{\nu}}\right)$ it used the experimental value produced by A.J Bard and L.R Faulkner for obtaining the $\psi(\Delta E_p)$ function and convert it to $\psi\left(\frac{1}{\sqrt{\nu}}\right)$ [10].



Eventually, the K_s parameters were calculated from the slope of the ψ vs. $(\frac{1}{\sqrt{v}})$ curves.

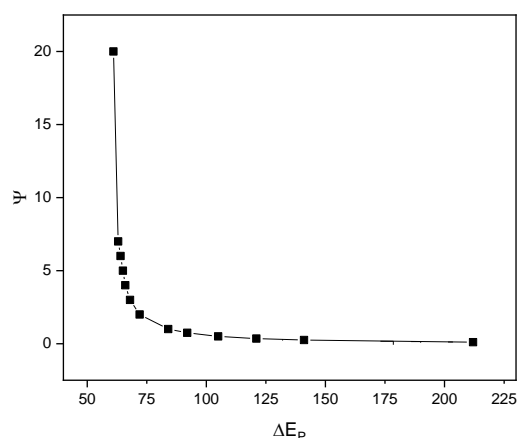


Figure 3: dependence of the dimensionless rate parameter from the voltammetric behavior (ψ) on the peak potential separation (ΔE_p).

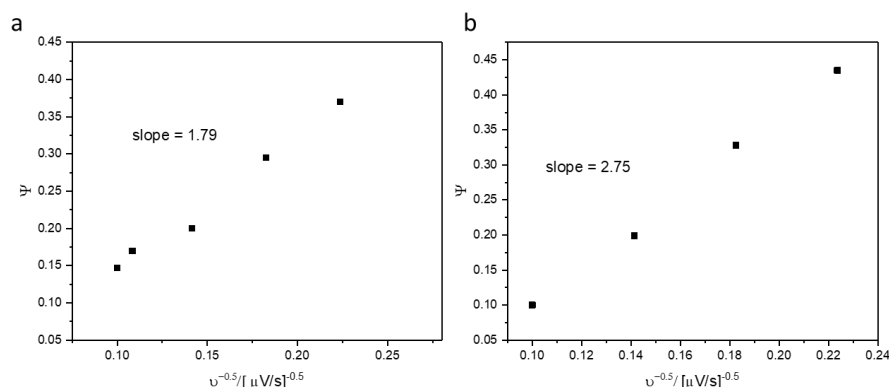


Figure 2.4: dependence of the dimensionless rate parameter of the voltammetry behavior (ψ) on the scan rate $(\frac{1}{\sqrt{v}})$. The calculations belong to the processes related to peaks c (Figure 2.1), namely, the most pronounced Mg ions intercalation (the second stage). Chart a, b relates to ICD and APC solutions, respectively.

It is important to note that the heterogeneous rate constants for the charge transfer processes across the electrodes interfaces were calculated only for **peak c**, since the other peaks appears too broad in the CVs obtained and does not allow to determine the exact peak potential (necessary for the calculations) precisely.

According to this model the heterogeneous rate constant for the charge transfer across the electrodes/solutions interfaces were found as 9×10^{-10} and 1.4×10^{-9} cm/s for ICD and APC solutions, respectively. This finding reveals that the charge transfer processes across the electrode's interfaces are faster in APC than in ICD solutions. This is well understood in light of higher interactions of Mg ions with DME compared to THF solutions (concluded from a previous work) [9].

This suggests that **the electroactive species in rechargeable magnesium systems may have an important impact on the electrochemical characteristics of the cells by influencing the interfacial electrochemical processes**. The diffusion coefficient though, as long as naked Mg ions are inserted into the cathode hosts, remains solutions invariant.



2.5. Conclusions:

The research described above deals with important questions about the electroanalytical and solid-state electrochemical response of magnesium ions interacting with copper containing Chevrel phase cathodes. It studied, qualitatively and quantitatively, the influence of the electrolyte solutions identity and structure on critical features of CP cathodes' electrochemical processes. These include thermodynamic properties, RDS, diffusion coefficients, heterogeneous rate constant for charge transfer across the electrodes interfaces and some other general features. For this purpose, we compared the electrochemical response of $\text{Cu}_{0.09}\text{Mo}_6\text{S}_8$ in two important electrolytes solutions, $\text{PhMgCl}/\text{AlCl}_3/\text{THF}$ and $\text{MgTFSI}_2/\text{MgCl}_2/\text{DME}$.

It has shown that some general features, such the formal potential for the intercalation/de-intercalation processes are strongly affected by the electrolyte solutions identity. The intercalation process of Mg ions into $\text{Cu}_{0.09}\text{Mo}_6\text{S}_8$ electrodes occurs at higher potential in APC than in ICD solutions. This shows that for practical applications the choice of electrolyte solution may have a great impact on the cells' energy density, even upon using identical electrodes. In addition, the electroactivity related to the Cu residues in the host is also affected by the electrolyte solutions identity. These electrochemical processes, associated with Mg-Cu displacement, are thermodynamically favorable and kinetically faster in ICD than in APC solutions.

We also found that the rate determining steps related to different electrochemical stages during Mg intercalation are affected by the electrolyte solutions. The most important Mg ions intercalation step into $\text{Mg}_x\text{Mo}_6\text{S}_8$ (related to **peak c** in the CVs, **Figure 2.1**) exhibits a quasi-equilibrium behavior at low scan rates in APC solutions.

The same stage in ICD solutions though, has a semi-infinite diffusion limited process character even at the slowest scan rates. On the other hand, process a, associated with electrochemical reaction of Mg-Cu assemblies, exhibits quasi-equilibrium step in ICD solutions, while in APC solutions the process is semi-infinite solid-state diffusion controlled.

3. TFSI containing electrolyte solution effects on high voltage cathode electrochemical activity in rechargeable magnesium batteries

Before diving into the focused study, the electrochemical activity of the thin, monolithic V_2O_5 films, deposited on Pt foil electrodes was characterized with Li-based solution. Not only Li ion activity with the oxide is a well-studied and serves as excellent benchmarking system, it is also very forgiving to the experimental conditions, in particular to passivation.

Figure 3.1a presents the cyclic voltammograms of V_2O_5 thin film electrodes in LiTFSI/ACN and $\text{LiClO}_4/\text{ACN}$ solutions. By analyzing these voltammograms two important insights can be deduced. The first related to the crystal structure and the mass loading of the host. The second related to the effect of the anion on the intercalation process of Li^+ into the V_2O_5 . The electrochemical signatures point that the deposited V_2O_5 unequivocally assumed the α -phase crystal structure, with orthorhombic unit cell structure. Raman spectra gave further support to this notion. The electrochemical response also clearly reflects the facile intercalation/de-intercalation processes (rates), as well as some insights about the thermodynamics (charge/intercalation levels, voltages) and phase transitions (sharp current peaks).

The redox peaks are located at the same potentials and the current densities, and the charge transferred during the intercalation is practically identical in both systems. These results indicate, unequivocally, that the electrochemical intercalation process of Li^+ ions with V_2O_5 is indifferent to the anion identity. Not at the thermodynamic level, (reaction potentials) and not at the reaction kinetics (current densities).

In stark difference from the Li-based solutions, it was found that the electrochemical response of V_2O_5 in Mg-ion based solutions is strongly affected by the anion in the electrolyte solution. **Figure 3.1b** shows the cyclic voltammograms of thin film V_2O_5 electrodes in $\text{Mg}(\text{TFSI})_2/\text{ACN}$ and $\text{Mg}(\text{ClO}_4)_2/\text{ACN}$ electrolyte solutions. Here also the charge balance curves corresponding to the 1st and the 3rd cycles inserted. The potential-current dependency provides important insights into the electrochemical reaction kinetics. At the macroscopic level, the currents



registered in the $\text{Mg}(\text{ClO}_4)_2/\text{ACN}$ are much higher than with in $\text{Mg}(\text{TFSI})_2/\text{ACN}$. This primary observation indicates that the overall intercalation kinetics of Mg ions into (and out of) V_2O_5 electrodes is strongly diminished due to the existence of the TFSI anion. Such strong effects may originate due to several reasons, like surface phenomena and solution structure differences.

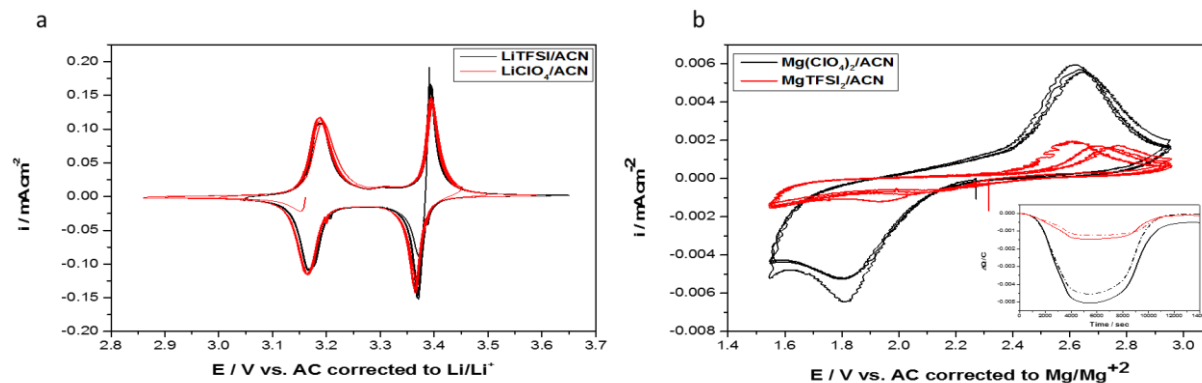


Figure 3.1: (a) Cyclic voltammograms of monolithic, thin film V_2O_5 electrodes in a three-electrode cell comprised of AC as counter and reference electrodes. Electrolytic solutions: LiTFSI/ACN (black line) and with $\text{LiClO}_4/\text{ACN}$ (red line). Scan rate of 1 mV s^{-1} @ RT. And (b) cyclic voltammograms of monolithic, thin film V_2O_5 electrodes in same three-electrode cell configuration with $\text{Mg}(\text{TFSI})_2/\text{ACN}$ (black line) and with $\text{Mg}(\text{ClO}_4)_2/\text{ACN}$ (red line) electrolyte solutions at a scan rate of 0.2 mV s^{-1} @ RT. Inset: the corresponding charge balance of the first (solid line) and the third (dashed line) cycles.

However, deeper analysis, at the microscopic level, is needed in order to get better understanding the mechanism underlying the anion effect on the intercalation of Mg ions into the V_2O_5 . The voltammograms of the $\text{V}_2\text{O}_5/\text{Mg}(\text{ClO}_4)_2/\text{ACN}$ system exhibits two redox peaks at -0.22 and 0.6 V vs. AC quasi reference electrode (1.88 and $2.7 \text{ V vs. Mg/Mg}^{+2}$).

The voltammograms of the $\text{V}_2\text{O}_5/\text{MgTFSI}_2/\text{ACN}$ system exhibited weak and poorly resolved, extremely broad, reduction peak. This reflects poor intercalation kinetics into the oxide lattice. An additional interesting observation stands up when looking at the corresponding oxidation peaks of this system. The very first oxidation peak is located exactly at the same potential as the one for $\text{V}_2\text{O}_5/\text{Mg}(\text{ClO}_4)_2/\text{ACN}$. However, at the following cycles, the oxidation peak is shifting to ever increasing voltage. In other words, higher overpotential is developing after each cycle. Interestingly, the increase in the oxidation peak voltage occurs only from the second cycle and on. Namely, the first oxidation peak is not shifted to higher potentials (relative to the CV in perchlorate), indicating that biasing to lower potential does not cause such peak potential shift. At the same rate, the ever-increasing oxidation peak potential is strongly associated with the positive biasing of the electrode cycle by cycle. Whatever this phenomenon origin is, it is associated with electrochemical oxidation processes rather than reduction, within the voltage window used in the study.

Based on the above results, it hypothesized that TFSI^- anions react at high voltages with V_2O_5 to form partially impermeable surface film which hampers the intercalation Mg^{2+} ions into the solid host.

To test the hypothesis, it carried out the following experiment. A V_2O_5 electrode was electrochemically treated in TFSI-based solution. The electrochemical treatment involved single step chronoamperometry measurement to 0.8 V vs AC to 10 hours in $\text{MgTFSI}_2/\text{ACN}$ electrolyte solution. The electrochemical treatment, according to the hypothesis should bring the electrode's surface, in case it is indeed chemically affected by the TFSI, to be partially passivated. Then, the electrode was washed thoroughly and transferred to $\text{Mg}(\text{ClO}_4)_2/\text{ACN}$ solution, and several consecutive CV's were performed.

Figure 3.2 shows the CV curves for the V_2O_5 electrode in $\text{Mg}(\text{ClO}_4)_2/\text{ACN}$ after the electrochemical treatment in the TFSI-based solution. Interestingly, as can be clearly seen in **Figure 3.2**, the first cycles in the perchlorate solution resembles the CV's very much in TFSI solution. However, continuous cycling shows evolution of CV features, that are substantially stronger, and after 7 cycles resembles that very much for untreated electrodes cycles in perchlorate-based solutions. The treated electrode still exhibits intercalation kinetic limitation, as



observed by the washed-out negative half cycle current wave and the charge associated with the process do not reach that for untreated electrode.

The results reveal that the intercalation process from $\text{Mg}(\text{ClO}_4)_2/\text{ACN}$ solution becomes substantially sluggish after exposing the V_2O_5 to $\text{MgTFSI}_2/\text{ACN}$ solution, at high voltage of around 2.8V vs Mg/Mg^{2+} . In other words, the V_2O_5 cathode becomes practically blocked due to the electrochemical processing in TFSI-based solution. The results reveal that TFSI anions in the solution have negative effect on the electrochemical activity of V_2O_5 . Moreover, these negative effects are most probably due to formation of impermeable surface film as a result of TFSI oxidation. The improvement in the electrochemical response during cycling in the perchlorate solution can be explained on the grounds of dissolution or breaking of this thin, passivating surface film. The mechanism of this de-passivation process is unclear yet.

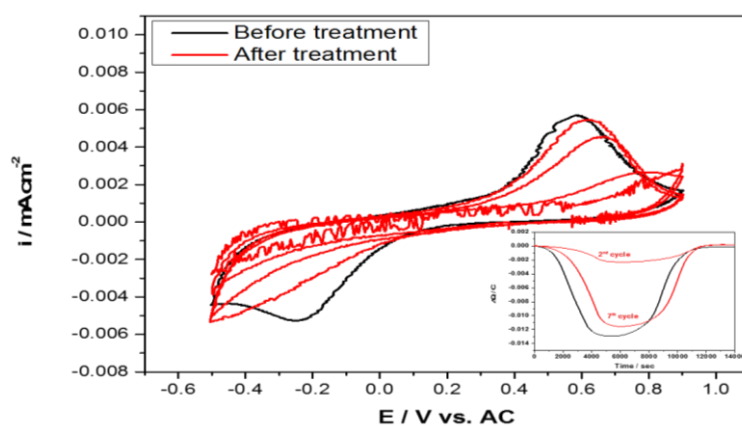


Figure 3.2: the 2nd cyclic voltammogram curves of monolithic thin film V_2O_5 in three electrode cells with $\text{Mg}(\text{ClO}_4)_2/\text{ACN}$ before (black line), and the 1st, 2nd, 4th and 7th cycles after electrochemical treatment in $\text{Mg}(\text{TFSI})_2/\text{ACN}$ solution (red line). Scan rate was 0.2 mV s^{-1} . Inset: the corresponding charge balance for the 2nd cycle of the untreated (black line) and the 2nd and 7th cycles for treated electrode (red line).

Despite the strong evidences for the negative effect of the TFSI anions on the intercalation process of Mg ions into V_2O_5 host, electrochemistry is not sufficient to elucidate the mechanisms associated at the chemical level. In order to get deeper understanding at the molecular and morphological levels, complementary spectroscopic and microscopic methods were employed.

Figure 3.3 shows the results of XPS analysis for V_2O_5 electrodes after 12 CV cycles in $\text{Mg}(\text{ClO}_4)_2$ and MgTFSI_2 based electrolyte solutions. The XPS spectra indicate that there are some differences in the surface chemistry of the V_2O_5 electrodes processed in the two solutions. The XPS spectra of both systems exhibit peaks around 285 eV associated with carbon C 1s. The smaller, asymmetric peaks at around 289 eV can be identified as carboxylates. In any case, both qualitatively and quantitatively the C 1s spectra are virtually the same for both cases.

Both samples exhibit Mg 2p peaks associated with an oxidized form of Mg. Quantitatively, the contribution of this peak is larger for the sample cycled in perchlorate solution, compared with the TFSI. Qualitatively, the two Mg 2p features, for the two samples, look very similar. Unfortunately, the S/N ratio is too large to enable intricate qualitative information regarding the Mg chemical environment.

The most important peaks are found around 685.8 eV, indexed to F 1s. This peak reflects the critical difference between the samples and sheds light on the electrochemical results. These peaks were observed, naturally, only in electrodes that were electrochemically processes in $\text{MgTFSI}_2/\text{ACN}$. From the F 1s binding energy, these peaks are associated with inorganic fluorine anion, in conjunction with electropositive metal cation. The peak position, 685.8 eV, precludes the likelihood of organic-based fluorine, such as CF_3 moiety. It believes that this peak testifies for the formation of insoluble and Mg-ion impermeable MgF_2 as a very thin surface film.

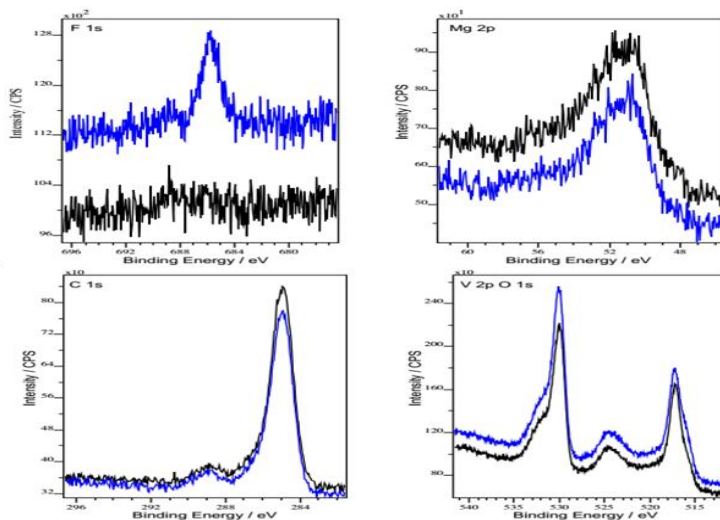


Figure 3.3: XPS data obtained from measurements of monolithic thin film V_2O_5 electrodes after 12 CV cycles in $Mg(ClO_4)_2/ACN$ (black line) and in $MgTFSI_2/ACN$ (blue line) electrolyte solutions. F, Mg, C, V and O spectra are presented.

Further insights about the surface nature of the electrodes after electrochemical treatment may be provided by HR-SEM measurements. **Figure 3.4** shows HR-SEM images of pristine V_2O_5 electrode, and V_2O_5 electrodes after 6 CV cycles in $Mg(TFSI)_2/ACN$ and $Mg(ClO_4)_2/ACN$ electrolyte solutions. The HR-SEM micrographs clearly indicate that the surfaces morphology of the pristine sample is slightly different from the ones electrochemically cycled. The cycled electrodes show somewhat smoother and larger crystallite surfaces, and larger cracks. It does not know yet what causes this difference. While the general morphology of the samples that were cycles in the two electrolytic systems is very similar, there is a very profound difference, with critical consequences.

The electrodes cycled in $Mg(ClO_4)_2/ACN$ are clean from impurities, and only some of the crystallites edges show whiter colour, associated with slight charging effects. Similar features are observed also with the pristine electrode, but to a lesser extent. In contrary, the surface of the V_2O_5 cycled in $MgTFSI_2/ACN$ comprises of lots of large islands of areas that show stronger charging effects. It is also possible to discern that the surface morphology of these areas exhibit kind of grainy or spongy texture. Due to the decreased electronic conductivity associated with these islands, it is practically impossible to acquire micrographs at much larger magnification (charging). Hence, it is hard to determine accurately this surface layer's nature. Obviously, they are very thin. Interestingly, the same kinds of surface features were also found on V_2O_5 electrodes that were cycled in LiTFSI solutions; however, in this case the islands were smaller.

The above findings strongly support the hypothesis of formation of thin, passivating layer, when V_2O_5 electrodes are cycled in TFSI-based solution.

It is well known that even an exceedingly thin over-layer deposit of stable film may cause serious impedance for Mg intercalation, and even complete passivation. Any single analytical technique on its own cannot provide the needed robust evidence as to the origin of the sluggish electrochemical process of magnesium intercalation in the TFSI based electrolyte solution. However, the results from the electrochemical measurements, coupled with the XPS surface elemental analyses and HR-SEM images leads to the unambiguous conclusion that TFSI anion reacts electrochemically with V_2O_5 electrodes to form impermeable/semi-permeable surface films which hampers the electrochemical insertion of Mg ions into the oxide host. The chemical analysis supports the hypothesis that this surface film is composed of mainly MgF_2 . However, the reaction mechanism yielding to this surface film is not clear yet.

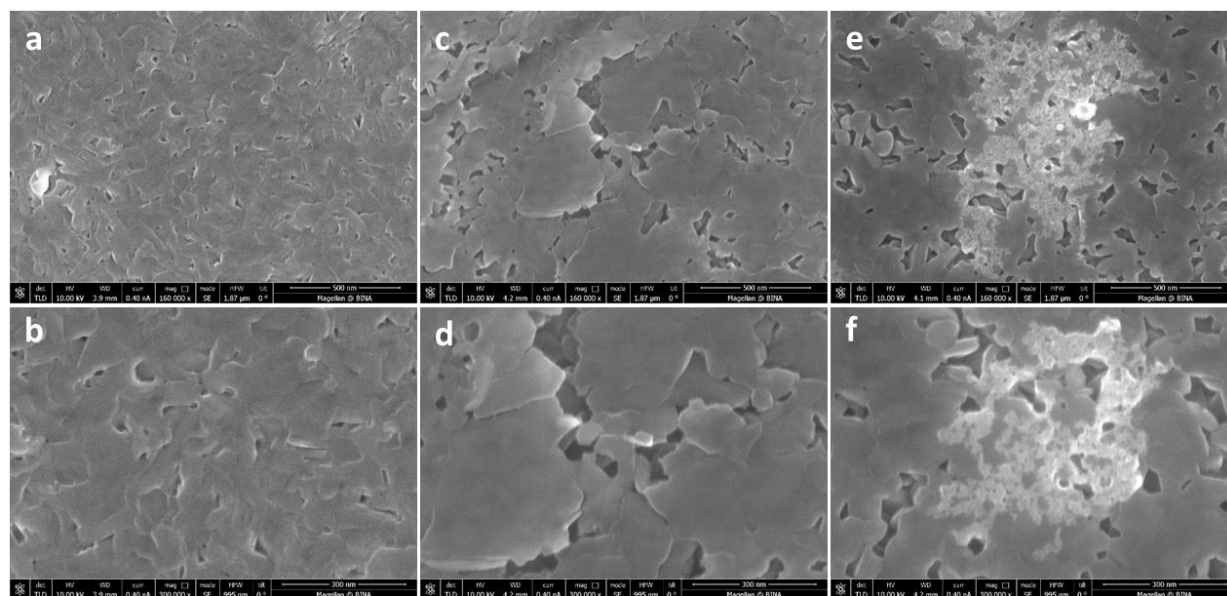


Figure 3.4: HR-SEM images of pristine, monoclinic V_2O_5 thin film electrodes (thickness ~ 30 nm) (a,b) and after 6 CV cycles at a scan rate of 0.2 mV/s in $Mg(ClO_4)_2/ACN$ (c,d), and $Mg(TFSI)_2/ACN$ (e,f) electrolyte solutions.

4. Solvent effects on the reversible intercalation of Mg ions into V_2O_5 electrodes.

4.1. Non- aqueous magnesium electrochemistry – the effect of the presence of DME in ACN solutions on the electrochemical performances of V_2O_5 electrodes

At the first step, the electrochemical response of the V_2O_5 electrodes was examined by CV in 0.25M $Mg(ClO_4)_2/ACN$ electrolyte solution. Since it wanted to work in the reversible intercalation window of the material, we selected the potential range between -1.72 and 2.87 V vs Mg/Mg^{2+} . Before starting the measurements and after stabilization time, the OCV of the working electrode found to be 0.15V vs. AC (2.27 V vs Mg/Mg^{2+}). **Figure 4.1a** shows the CV curves of the 1st and the 2nd cycles of the thin film V_2O_5 electrodes at a scan rate of 0.2mV/s. The voltammograms exhibit two broad redox peaks at -0.2 V (and 0.56 V vs. AC (2.68 V and 1.92 V vs. Mg/Mg^{2+}).

Although the V_2O_5 electrodes undergo reversible insertion of Mg^{2+} ions, as can be concluded from the curves, a relatively large potential gap between cathodic and the anodic processes is suspected to reflect kinetic limitations. The kinetic limitation may result from the intrinsic low solid-state diffusion of magnesium ions, as measured in most of the solid hosts. Alternatively, it may be due to slow interfacial charge transfer. Obviously, the two proposed kinetic control mechanisms may be additive under some circumstances.

Figure 4.1b demonstrates a typical chronopotentiometric curve of V_2O_5 electrodes at a current density of $0.2\mu A\ cm^{-2}$ in the potential range of -0.1 and 0.3V vs. AC quasi-reference. It should be noted that the cut-off potentials were -0.4 and 0.3V vs. AC during discharge and charge, respectively, a much narrower range than those used the CV measurements.

The slow (low current density) galvanostatic cycling allowed using this narrow voltage range for nearly full 0.5 electrons per unit, compared with the CV, as much lower IR drops plagued the electrochemical processes. Nevertheless, during the discharging stage, the system was limited to deliver no more than 0.45 Mg ions per unit of charge (90% DOD) in order to keep the system within safe limits for a fully reversible process. The galvanostatic curve exhibits a midpoint voltage for discharge and charge of 0.0V and 0.22V vs. AC, (2.12 V and 2.34 V vs Mg/Mg^{2+}), respectively.

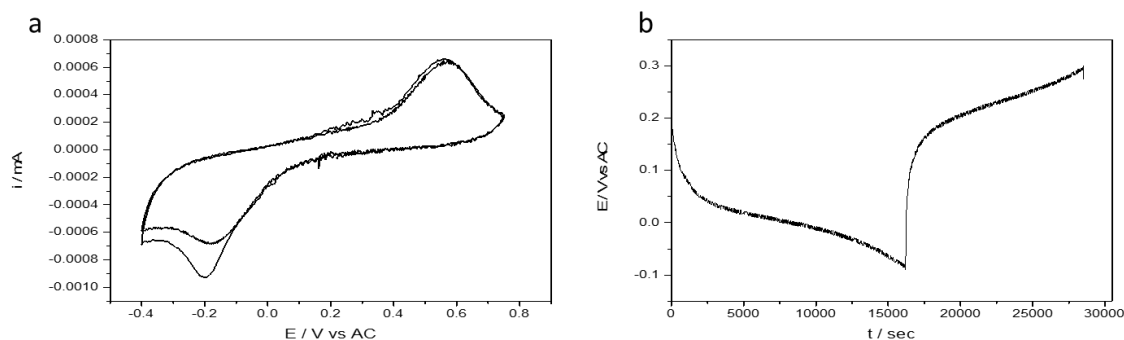


Figure 4.1: (a) cyclic voltammogram at scan rate of 0.2 mV s^{-1} and (b) galvanostatic charge/discharge curve at a current density of $0.2 \mu\text{A cm}^{-2}$ for thin film V_2O_5 cathodes in three electrodes cell. AC electrodes served as counter and reference electrodes. $\text{Mg}(\text{ClO}_4)_2/\text{ACN}$ as the electrolyte solution.

Figure 4.2 shows the electrochemical behaviour of V_2O_5 in $\text{Mg}(\text{ClO}_4)_2/\text{DME}:\text{ACN}$ 1:1 v% electrolyte solution during potentiostatic and galvanostatic measurements. The OCV of the working electrodes in this system was found to be 0.12V vs. AC. The experimental parameters for the CV and for the galvanostatic measurements were set to be identical to those used for the experiments with ACN solutions. An immediate observation is that the current response in the CV during the cathodic half cycle commences and occurs at lower voltages compared to the same process in pure ACN/ $\text{Mg}(\text{ClO}_4)_2$.

It hypothesizes that above mentioned behaviour stems from a higher degree of kinetically limitations imposed by the DME in the ether containing solution. This effect of DME should not be attributed to Mg solid-state diffusion within the host (cannot be affected by changes in the solution phase), but rather it relates to inhibiting interfacial processes. The sluggish kinetics of the cathodic process (Mg ions intercalation) due to the presence of DME is most likely related to one of the following possibilities: slow charge transfer, slow desolvation, or parasitic reactions and formation of surface films. The chronopotentiometry measurements show that the midpoint voltage for Mg ions insertion from DME containing electrolyte solution is -0.14 V vs. AC, while the midpoint voltage for de-insertion is 0.17 V vs. AC.

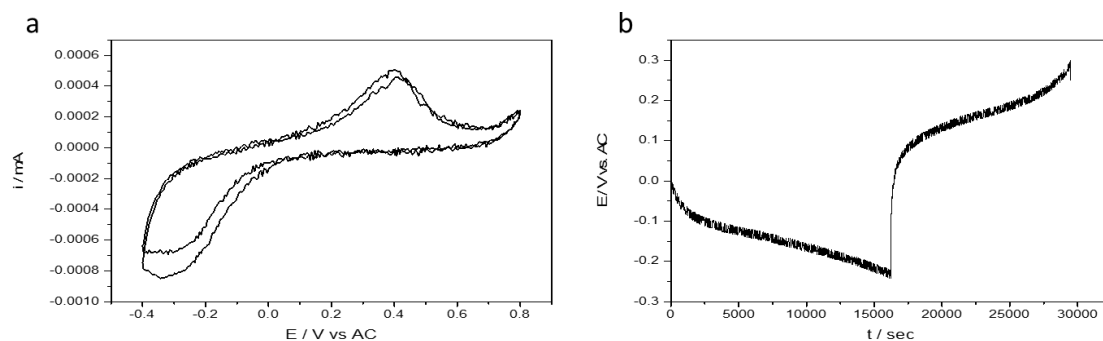


Figure 4.2: (a) cyclic voltammograms at a scan rate of 0.2 mV s^{-1} and (b) galvanostatic charge/discharge curve at current density of $0.2 \mu\text{A cm}^{-2}$ for thin film V_2O_5 in three electrode cell composed containing AC counter and reference electrodes. $\text{Mg}(\text{ClO}_4)_2/\text{ACN}:\text{DME}$ 1:1v% electrolyte solution.

In order to assess the effect of DME as a solvent on the electrochemical insertion of Mg^{2+} ions into V_2O_5 cathode (orthorhombic phase), it summarized the results of the electrochemical study in a comparative form.

Slow scan rate cyclic voltammetry may be useful for thermodynamic assessments, while fast scan rates, such as those used in this study, may shed light on the kinetic aspects of the processes during electrochemical



intercalation and de-intercalation. **Figure 4.3** compares the cyclic voltammetry and galvanostatic charge-discharge curves of V_2O_5 electrodes in $Mg(ClO_4)_2/ACN$ and $Mg(ClO_4)_2/DME:ACN$ 1:1v% electrolyte solutions.

The cyclic voltammogram curves depicted in **Figure 4.3a** clearly show the negative impact of DME addition on the rate of the cathodic process. In pure ACN based electrolyte solution the current response is observed at higher potentials (lower overpotential) during intercalation, than that measured with the DME:ACN electrolyte solution. These results reflect insertion kinetics hurdles for Mg ions in DME containing solutions, compared to pure ACN. In addition, the CVs signature of the V_2O_5 electrodes in ACN:DME based electrolyte solution exhibits much wider cathodic peaks, what supports the hypothesis of limited insertion kinetics compared to that in the pure ACN based electrolyte solution.

Surprisingly, as observed in the CV response of the electrodes, the anodic current peak obtained in the pure ACN based electrolyte solution is centered at higher potentials than the one measured in DME containing solution. Along with the hypothesis of interfacial kinetic influence of the solvents, it is consistent with more energy penalty (E_a) for the Mg^{2+} extraction from the solid host to pure ACN electrolyte solution compared with the DME-containing one.

Additional support to the hypothesis is obtained from the slower, galvanostatic experiments. **Figure 4.3b** which shows the galvanostatic charge-discharge voltage profiles for the V_2O_5 electrodes in the two electrolyte solutions, at a current density of $0.2 \mu A cm^{-2}$. The chart shows clearly that intercalation of Mg ions into V_2O_5 electrodes in the DME containing solution is harder compared to that occurring in pure ACN solutions (lower voltage profile for the former case, the red curve). In turn, de-intercalation of Mg ions from V_2O_5 electrodes is somewhat easier in the former case as reflected by the lower voltages at which Mg ions are de-inserted in the DME containing solution compared to the case of pure ACN solutions (higher voltage profile for the charging process, black curve in **Figure 4.3b**).

The sluggish kinetic intercalation of Mg^{2+} into V_2O_5 in the presence of DME can be explained by three different mechanisms:

- 1) DME- Mg^{2+} interactions form very stable solvates. These casts large energetic penalty during the desolvation stage and slows down the insertion of Mg ions into V_2O_5 . The desolvation toll associated with the less coordinating solvent, ACN, is smaller and thus exhibits faster intercalation kinetics, at lower overpotentials.
- 2) The intercalation process is slowed in the DME-containing solution due to surface film formation on the cathode.
- 3) For some reason, e.g. DME-co intercalation, the solid-state diffusion of the magnesium ions is slower.

The first two scenarios suggest a slowdown of ionic charge transfer across the electrodes interface. Either Mg^{2+} ions migration through interfacial surface layers or solvation shell stripping from Mg ions near the electrode's interface are energy and time-consuming processes. Co-insertion with a relatively large solvation shell should affect the solid-state diffusion rate, and thus the overall intercalation/de-intercalation kinetics, albeit with unpredictable direction and magnitude. However, the general similarity observed in the electrochemical responses of the electrodes measured with the DME-free and DME-containing electrolyte solutions, suggests that the presence of DME in solutions does not change the basic solid-state Mg ions diffusion mechanism the V_2O_5 hosts. The asymmetry in the DME effect on Mg ions insertion and de-insertion, namely, slowing down intercalation but facilitating de-intercalation, points out against the second mechanism. If transport through surface layers would play a role as an impedance factor, the slowdown effect on insertion and de-insertion processes should be very similar.

Figure 4.3c compares voltage profiles of V_2O_5 electrodes in prolonged galvanostatic discharge processes corresponding to nearly 1 electron transfer per V_2O_5 molecule, in DME containing and DME-free solutions. The comparison between the solutions in long-term experiments as presented in **Figure 4.3c**, emphasizes further the negative effect of the presence of DME in solutions on the intercalation process of Mg ions into the V_2O_5 electrodes: In order to fully discharge the V_2O_5 cathodes in the presence of DME (up to one electron and half Mg ion per V_2O_5 unit), much lower potentials (excessive energy toll) have to be applied under the same experimental conditions. The over-potential for insertion increases with the depth of discharge in the ACN:DME based



electrolyte solution while in the ACN based solution the over-potential for Mg insertion reaches almost steady-state values.

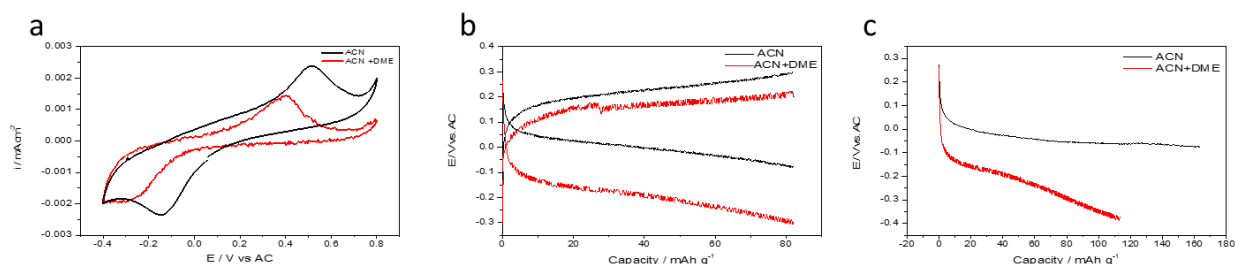


Figure 4.3: Comparative study of thin layer, monolithic V_2O_5 electrodes in $Mg(ClO_4)_2/ACN$ based electrolyte solutions without (black line) and with DME (red line). Cyclic voltammograms at scan rate of 0.2 mV s^{-1} (a) Typical voltage profiles of steady state cycles in galvanostatic cycling experiments at a current density of $0.2 \mu\text{A cm}^{-2}$ (b) Voltage profiles measured during prolonged galvanostatic discharge processes corresponding to nearly 1 electron and half Mg ion transfer per V_2O_5 molecule ($0.2 \mu\text{A cm}^{-2}$) (c).

In order to exclude the possibility of solution composition impact on the electrodes bulk behaviour, it calculated the diffusion coefficient of Mg ions in V_2O_5 using galvanostatic intermittent titration technique (GITT). GITT is a well-established technique for probing solid state diffusion coefficient of intercalants in hosts as a function of the electrode's potential and its state of charge (i.e. Mg ions contents). This technique may provide precise information only for single phases (i.e. solid solution-type intercalation products). Nonetheless, apparent diffusion coefficients calculated from GITT may still provide valuable comparative information about the Mg^{2+} ion transport properties in the solid host as a function of the solution composition.

Figure 4.4 shows curves obtained by applying GITT to the thin, monolithic V_2O_5 electrodes in DME-free ACN and DME-containing solutions. Each sequence was composed of 1 h of galvanostatic discharge at a current density of $0.1 \mu\text{A cm}^{-2}$ followed by an OCV measurement period of 1 h. The use of such long steps was necessary due to the relatively slow processes.

In this study, we calculated the apparent solid-state diffusion coefficient in order to assess it, and how the presence of DME affects the solid-state Mg^{2+} diffusion coefficient in V_2O_5 . Marked differences in solid-state diffusion coefficients should indicate substantial differences in the intercalated species (e.g. free Mg^{2+} ions or solvent co-intercalated Mg ions). The solid-state diffusion coefficients were calculated from the edges of the relaxation curves using Equation 4.

In Equation 4, the first part of this mathematical expression can be replaced by a constant, as all these parameters were kept identical in all experiments. Moreover, in the case of monolithic, thin film electrodes, this expression can be evaluated very precisely based on geometry, with roughness factor corrections if needed.

The results reveal that the apparent solid-state diffusion coefficient for the Mg ions in the host material is very similar for the two electrolyte solutions: 5.8×10^{-15} and 4.3×10^{-15} for the ACN and ACN:DME systems respectively. This result indicates that the solution species don't have any effect on the solid-state diffusion kinetics. This strongly supports the hypothesis that the Mg ions are inserted into the solid host as naked ions, devoid of solvation shell. This leaves the two other possible interfacial phenomena mentioned above, as factors that lead to the sluggish intercalation kinetics observed (well reflected in the charts of **Figures 4.1 – 4.4**).

As proposed before, the sluggish kinetic interfacial process may be attributed to either stripping the Mg ions from their DME-Mg solvation structure, or due to SEI-like surface films.

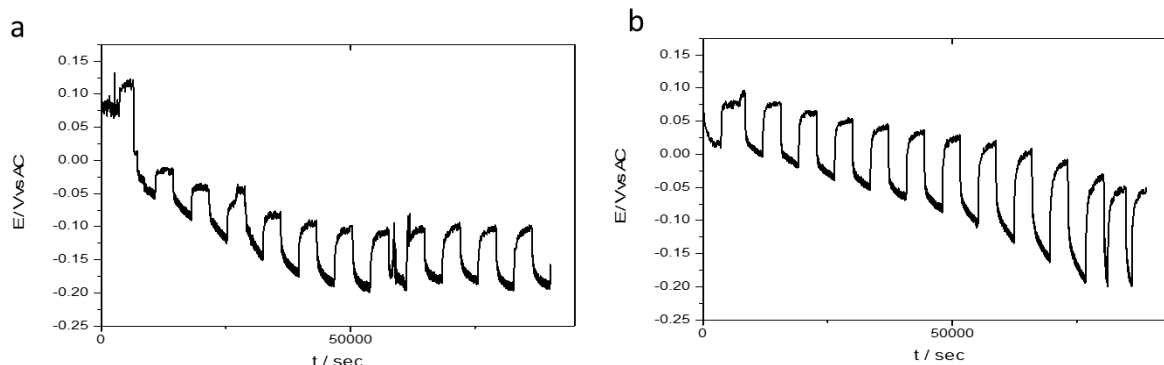


Figure 4.4: Galvanostatic intermittent titration technique (GITT) curves for V_2O_5 electrodes in ACN based electrolyte solution (a) and in ACN:DME based electrolyte solution (b).

4.2. Solutions structure – solvation effects

Study of the solutions structure by Raman spectroscopy was conducted in order to examine the hypothesis that DME interacts very strongly with the magnesium ions, expelling ACN molecules from the solvated ions and forming more stable solvated ions. Stable structure of cations in DME containing solutions may require large energy toll for their insertion as free ions into a solid host like V_2O_5 , compared to the situation in single solvent ACN solutions.

Figure 4.5 shows the Raman spectra of ACN, DME, 0.5M $Mg(ClO_4)_2/ACN$, 0.5M $Mg(ClO_4)_2/ACN$ -DME 1:1 and 0.5M $Mg(ClO_4)_2/ACN$ /1.5M DME solutions over the range of 200-2500 cm^{-1} . The most informative spectral regions are the 320-440, 2175-2350 and 800-900 cm^{-1} .

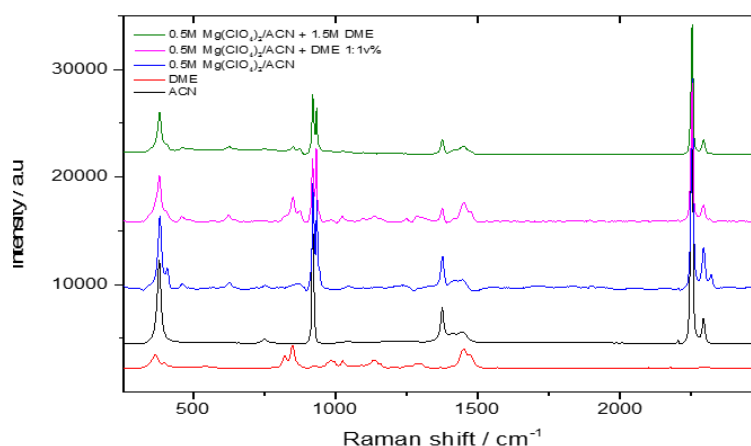


Figure 4.5: Raman spectra of pure ACN (black), pure DME (red), 0.5M $Mg(ClO_4)_2/ACN$ (blue), 0.5M $Mg(ClO_4)_2/ACN$ -DME 1:1v% (purple) and 0.5M $Mg(ClO_4)_2/ACN$ +1.5M DME (green).

The spectral information extracted from these regions shows that ACN and DME exist in two main forms: free or coordinated to Mg^{2+} ions. The existence of these forms and the ratio between them can provide important insights about the solution structure and the affinity of DME and ACN to the Mg ions. In addition, it may shed light on the effect of DME addition on the electrochemical intercalation of Mg^{2+} into V_2O_5 . The spectral data of the free and coordinated ACN and DME is presented in **Table 4.1** and **4.2**, respectively.



Table 4.1: observed frequencies of free and Mg^{2+} -coordinated CH_3CN

| Description | Pure ACN | $Mg(ClO_4)_2/ACN$ | | $Mg(ClO_4)_2/ ACN:DME 1:1 v\%$ | |
|---------------------------|----------|-------------------|--------------|--------------------------------|--------------------|
| | | Free | Coordinated | Free | Coordinated |
| $\nu_2 C\equiv N$ str | 2254 | 2256 | 2294 2321 | | |
| $\nu_4 CC$ str | 919 | 921 | 945 | 919 | - |
| ν_3 | 1375 | 1375 | - | 1375 | - |
| Comb ($\nu_{3+} \nu_4$) | 2294 | 2294 | 2294 2320 | 2294 | - |
| $\nu_8 C-C\equiv N$ band | 380.5 | 383 | 409 | 383 | 403(low intensity) |

Table 4.2: Observed Raman shifts for free and Mg^{2+} -coordinated DME in the different solutions.

| Description | Pure DME | | $Mg(ClO_4)_2/ACN$ | $Mg(ClO_4)_2/ ACN:DME 1:1 v\%$ | | $Mg(ClO_4)_2/ACN + 1.5M DME$ | |
|-----------------|----------|----------------------|-------------------|--------------------------------|----------------------|------------------------------|----------------------|
| | Position | Normalized intensity | Position | Position | Normalized intensity | Position | Normalized intensity |
| DME-free | 822 | High | - | 820 | low | 818 | low |
| 3DME: Mg^{2+} | - | | - | 875 | High | 875 | High |

Figure 4.6 presents the 2175-2350 cm^{-1} region of the Raman spectra of the different solvents and electrolyte solutions. This region contains three important peaks. The peak at 2256 cm^{-1} is attributed to $\nu_2 C\equiv N$ stretching band of the free ACN in the $Mg(ClO_4)_2$ electrolyte solutions (2254 cm^{-1} in pure ACN). The peak at 2294.3 cm^{-1} exists in all the electrolyte solutions and in the pure ACN spectra also. This peak is attributed to $\nu_3 + \nu_4$ combination band of free ACN and is also associated with the $\nu_2 C\equiv N$ stretching of Mg-ions coordinated by ACN.

Interestingly, the intensity of these peaks decreases with the following order: $Mg(ClO_4)_2/ACN > Mg(ClO_4)_2/ACN:DME 1:1v\% = Mg(ClO_4)_2/ACN+1.5M DME > pure ACN$.

These results indicate that Mg-DME interactions are thermodynamically preferable compared to that of ACN-Mg. So, even at the precise stoichiometric amount of DME (3 DME molecules per 1 Mg ion), the ACN-Mg bonds are replaced by the 3DME-Mg solvated structures. Interestingly, the free-ACN peak intensity is still low. This indicates for one of the three possibilities:

- 1) Not all the ACN-Mg bonds are replaced, even at high concentration of DME;
- 2) Fast exchange of ligands does occur between DME and ACN, possibly with leaving one of the DME ligands as a monodentate ligand; and
- 3) The interaction between the ACN and the cages of $Mg^{+2}DME_3$ is very strong.

The most informative peaks in this spectral region are located at 2321 cm^{-1} . This peak may be attributed to the $\nu_3 + \nu_4$ combination band of ACN coordinated to Mg^{2+} ions. As observed in **Figure 4.6**, this peak exists only in spectra of $Mg(ClO_4)_2/ACN$ solutions and is absent in DME containing solutions. This result provides very strong evidence for the stronger affinity of DME to Mg ions compared with that of ACN.

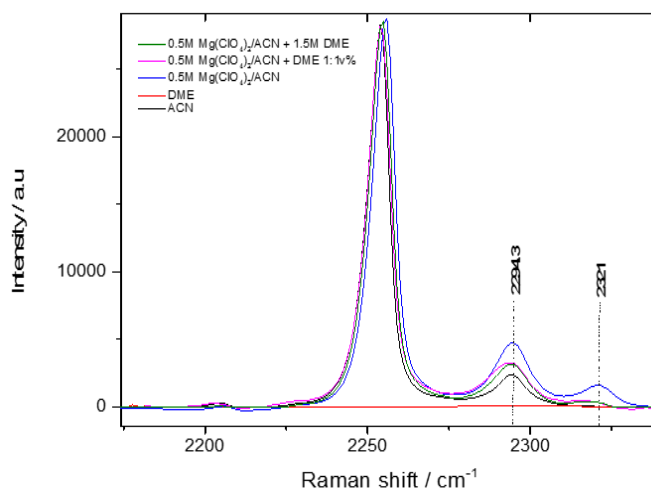


Figure 4.6: Raman spectra of pure ACN (black), pure DME (red), 0.5M Mg(ClO₄)₂/ACN (blue), 0.5M Mg(ClO₄)₂/ACN:DME 1:1v% (purple) and 0.5M Mg(ClO₄)₂/ACN+1.5M DME (green), in the 2175-2350 cm⁻¹ spectral region of.

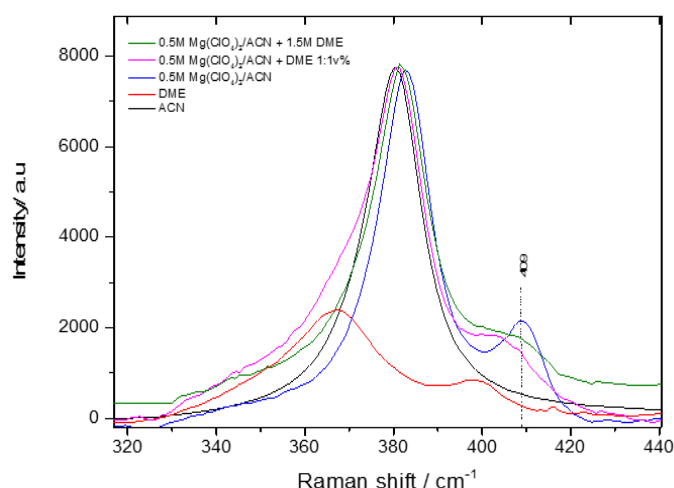


Figure 4.7: Raman spectra of pure ACN (black), pure DME (red), 0.5M Mg(ClO₄)₂/ACN (blue), 0.5M Mg(ClO₄)₂/ACN:DME 1:1v% (purple) and 0.5M Mg(ClO₄)₂/ACN+1.5M DME (green), in the 320-440 cm⁻¹ spectral region .

Figure 4.7 presents the 320-440 cm⁻¹ region for the Raman spectra of the various electrolyte solutions. The peak at 383 cm⁻¹ is attributed to ν_8 C≡N asymmetric bending of free ACN (380.5 cm⁻¹ for pure ACN). The spectrum of the Mg(ClO₄)₂/ACN solution exhibits relatively a sharp peak at 409 cm⁻¹, which may be attributed to ν_8 C≡N asymmetric bending of Mg²⁺ ions coordinated with ACN. The intensity of this peak also decreases sharply when DME is added. These results are in line with our conclusion that DME-Mg ions interactions are much stronger than ACN-Mg ions interactions.

The 800-900 cm⁻¹ region contains two important peaks, related to DME and DME-Mg²⁺ interacting species. This spectral region is presented in **Figure 4.8**. The peak at 820 cm⁻¹ is attributed to TTG conformers of free DME in the DME containing electrolyte solutions (822 cm⁻¹ in pure DME). The most important peak in this region is the one at 875 cm⁻¹. This peak is associated with the symmetric breathing mode of the three DME molecules encaging Mg²⁺ ions in DME based solutions. This peak is observed even at relatively low concentrations of 1.5M DME in 0.5M Mg(ClO₄)₂/ACN solution. In addition, the peak of the free DME at 822cm⁻¹ almost disappears in both DME based solutions that were studied herein.



These results also indicate that addition of DME to $\text{Mg}(\text{ClO}_4)_2/\text{ACN}$ solution, even at relatively low concentrations, results in replacing the 6 ACN solvating Mg^{2+} ions by DME molecules, what forms very stable $\text{Mg}^{2+}\text{DME}_3$ solvated cations.

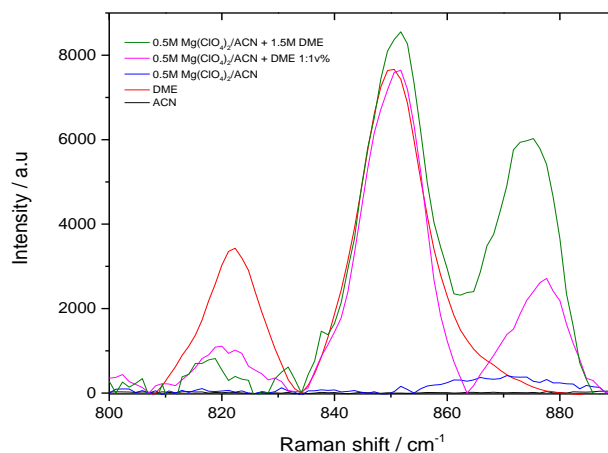


Figure 4.8: Raman spectra of pure ACN (black), pure DME (red), 0.5M $\text{Mg}(\text{ClO}_4)_2/\text{ACN}$ (blue), 0.5M $\text{Mg}(\text{ClO}_4)_2/\text{ACN}:\text{DME}$ 1:1v% (purple) and 0.5M $\text{Mg}(\text{ClO}_4)_2/\text{ACN}+1.5\text{M}$ DME (green), in the 800-900 cm^{-1} spectral region.

Hence, the above spectral studies provide very important insights about solution structures that can strongly affect the electrochemical behaviour of V_2O_5 electrodes in the Mg salt solutions that has been explored. As demonstrated above, when DME is added to ACN solutions, most of the $6\text{ACN}:\text{Mg}^{2+}$ solvated cation structures are replaced for the more stable $3\text{DME}:\text{Mg}^{2+}$ solvated cations. This means that stripping the Mg ions from the solvation cages containing 3 DME molecules requires higher energy than stripping the Mg from solvation shells of 6 ACN molecules. These results emphasize the ease of Mg ions de-solvation in solutions as an important factor that affects their intercalation into solid hosts.

4.3. Surface analysis

Ex-situ surface analysis was carried out in order to examine the possibility that cathode-related surface chemistry phenomena may be responsible to the slower intercalation of Mg ions into V_2O_5 electrodes in solutions containing DME.

The anodic stability of DME is documented in the literature, very similar to that of all other ether solvents (around 4 V vs. Li; 3 V vs. Mg). However, the electrochemical window of any solvent may be affected by the catalytic and electrocatalytic properties of the electrode.

In most studies, the DME electrochemical stability window was evaluated with Pt working electrodes. Electrochemical measurements were conducted in order to assess whether V_2O_5 has catalytic activity that may lead to DME decomposition at lower voltages than expected. Additionally, in such a hypothetical case the question is if there is a possibility of stable surface films formation onto the electrodes. Such surface films if formed may inhibit or slow down the insertion process of Mg ions into V_2O_5 hosts.

Figure 4.9 shows CVs of 0.25M LiBF_4/DME electrolyte solution with Pt and V_2O_5 working electrodes. LiBF_4 electrolyte was chosen due to its excellent anodic stability. Surprisingly, the DME exhibits higher anodic stability with V_2O_5 than with Pt. The current density for an onset of substantial oxidative electrochemical process was chosen to be 0.01 mA cm^{-2} . The anodic process of DME decomposition found to be at a potential of 4.3 V vs. Li/Li^+ (1.2V vs. AC), which is way above our working potentials range. Hence, electrochemical decomposition and surface film formation during the electrochemical measurements carried out in the present work is very unlikely.

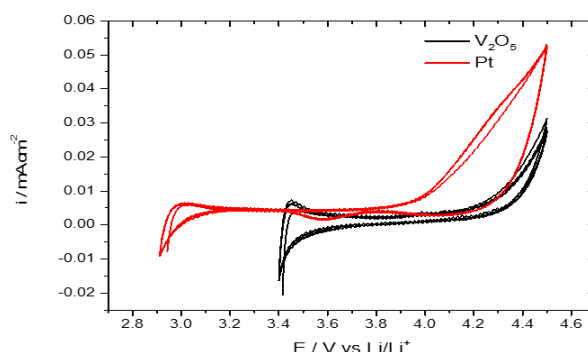


Figure 4.9: CVs measured with 0.25M LiBF₄/DME in three electrodes cells. Li electrodes served as counter and reference electrodes. Pt (red) and V₂O₅ (black) were the working electrodes. The anodic polarization started from the OCV and back.

However, this is not sufficient as concrete evidence against the existence of passivation phenomena in the V₂O₅ electrodes/solutions interface, as there is a possibility that spontaneous chemical (rather than electrochemical) reactions occur on the V₂O₅ electrodes surface in these solutions, resulting from the presence of DME. In order to clarify this possibility, we applied XPS measurements.

Figure 4.10a shows C 1s spectra obtained from a V₂O₅ electrode after 4 cycles in ACN:DME and in pure ACN based solutions. A reference spectrum obtained from a pristine V₂O₅ electrode is present as well. All spectra were calibrated by referring to the C 1s peak of the lowest binding energy (an instrument background signal). Both cycled and pristine V₂O₅ electrodes exhibited shoulders at around 287 eV which may represent adsorbed ethereal or alkoxy carbons. Most important is that the composition of the carbon species revealed by the XPS analysis show, to the most, only minor differences among the three electrodes. This suggests that no unique carbon-based surface films are developed on these three different samples.

Figure 4.10b shows the survey spectra of the V₂O₅ samples. All the three spectra exhibit peaks originating from V, Cl, O, Mg, C and N, and from the substrate, Pt. It can be simply observed from the survey spectra acquired from the three samples that the three electrodes exhibit very similar C 1s peak strength. The qualitative and quantitative data for all species detected by the XPS analysis testifies to only minor differences in the chemical surface composition of the samples. Quantification reports compared to the pristine V₂O₅ substantiate this conclusion.

Hence, the V₂O₅ electrodes do not develop any substantial surface passivation phenomena in these solutions. As expected from the anodic stability measurements (**Figure 4.9**), the presence of DME in solutions does not induce any unique surface phenomena.

All the above studies converge to the conclusion that the sluggish intercalation of Mg ions into V₂O₅ electrodes in the presence of DME is mainly due to kinetic issues related to solvation/desolvation phenomena.

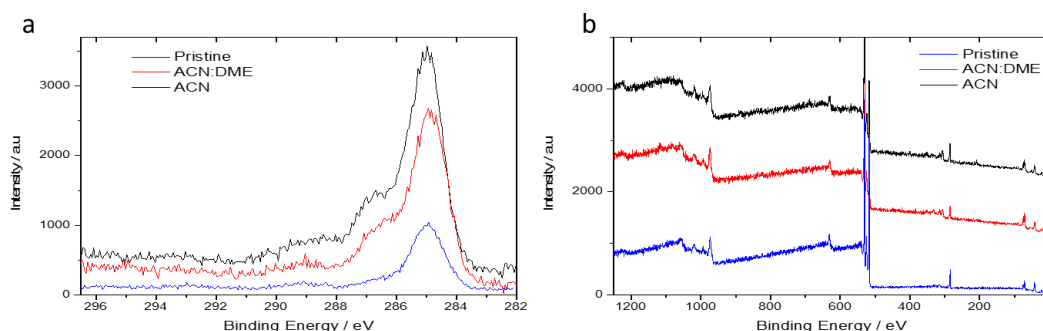


Figure 4.10: XPS emission spectra of thin film, monolithic V₂O₅ electrodes in ACN based electrolyte solution (black), ACN:DME based electrolyte solution (red), and pristine V₂O₅ (blue). (a) C1s emission peak, (b) survey spectra over wide binding energies range.



4.4. Conclusions:

The study described herein deals with an important topic, namely, the nature of Mg ions intercalation processes into hosts that can serve as cathode materials for rechargeable Mg batteries. While it has chosen very specific systems for this study they can be considered as very important and general models for rechargeable Mg batteries.

The cathode material used, V_2O_5 inserts reversibly Mg ions and thus can serve as a model for many oxide hosts that can be suggested as high capacity intercalation cathode materials for Mg batteries.

The basic electrolyte solution we used, $Mg(ClO_4)_2/ACN$ allows relatively smooth intercalation/de-intercalation processes of Mg ions into many transition metal oxides and sulfides. However, this electrolyte solution is not compatible with Mg metal anodes. DME is a solvent which solution allows reversible Mg deposition and dissolutions at high cycling efficiency. It has been found that the presence of DME in ACN based electrolyte solutions has a negative effect on the charge transfer kinetic across the V_2O_5 electrode/solution interface.

It examined possible manners in which DME in these solutions can influence badly the intercalation kinetics of Mg ions: Co-insertion with Mg ions, what slows down solid-state diffusion, surface phenomena which impeded interfacial charge transfer processes and impedance arising due strong solvation interactions which require high over-voltages in order to promote de-solvation. By calculating the diffusion coefficient for Mg ions insertion from GITT measurements we could eliminate the possibility of DME effect on the solid-state Mg ions transport.

By combinations of electrochemical and surface chemical studies (XPS), it eliminates the possibility of a negative effect of DME due to any kinds of surface films formation. By Raman spectroscopic studies it concluded that addition of DME into $Mg(ClO_4)_2/ACN$ solution results in replacing $ACN-Mg^{2+}$ ligands by more stable $3DME-Mg^{2+}$ solvated ions.

The electrochemical behavior of V_2O_5 electrodes in the presence of DME, coupled with the solutions structure study, indicates that the intercalation process of Mg cations is affected strongly by the formation of stable solvation shell with DME. Hence, de-solvation of these DME based structures impedes very strongly the intercalation of naked Mg ions into the vanadium oxide host.

It should be noted that ethers in general and glyme solvents like DME in particular are very important for the field of Mg batteries since they allow reversible behavior of Mg anodes. Thereby, addressing negative effects of ether solvents on the intercalation of Mg cations into cathodes due to strong solvation interactions, is interesting and important for the field of Mg electrochemistry in general and Mg batteries in particular.

5. The role of surface adsorbed Cl^- complexes in rechargeable magnesium batteries

In order to uncover the role of chlorides in the intercalation mechanism of Mg ions into Mo_6S_8 , Chevrel phase (CP), a careful set of electrochemical, structural, and spectroscopic measurements were conducted.

The first observation that drew attention to the decisive role of chlorides in Mg intercalation into CP was that the electrochemical response of CP in $MgTFSI_2/DME$ electrolyte solution, without $MgCl_2$, is awfully poor at RT. Similar results had been obtained also in $MgClO_4$ solutions in AN at RT. The poor reactivity of CP in these solutions is in stark contrast to numerous results obtained in a wide variety of Cl-containing solutions, including $MgTFSI$ in DME containing Cl^- (ICD).

In several experiments, each with new, fresh electrode and solution, it obtained some variations in the capacity results, ranging from almost zero to less than 30 mAh/g, in the first discharging process. In all cases, though, the discharging process was highly irreversible, and after few cycles the electrodes rendered completely inactive. **Figure 5.1a** show five consecutive CV cycles of CP in three electrodes cell containing Cl-free $MgTFSI_2/DME$. The CV signature is clearly evident of practically inactive CP. In addition, the CV response indicates that the electrochemical process is both kinetically and chemically irreversible. In contrast, when $MgCl_2$ is added to the solution (to yield "ICD" solution) the CV response shows fast and highly reversible Mg intercalation.



Moreover, in order overcome potential, unidentified initiation difficulties, the CP electrodes were polarized to different higher over-potentials and durations and cycled 5-15 times. In all cases the CP electrodes still showed poor electrochemical response in the absence of chlorides.

At this stage it held three main hypotheses about the role of Cl^- in the intercalation process of Mg ions into CP host;

- 1) **Surface passivation**; in Cl-free electrolytic solutions, some solution species (e.g. solvent, anions or trace contaminants, like water) decompose and accumulate onto the CP surface to form Mg-ions impermeable passivation film. Under this model Cl ions act as surface de-passivation agent by, e.g. dissolving the layer or inhibiting its accumulation in the first place. Similar model had been proposed also as to the role of Cl in allowing Mg deposition-dissolution from MgTFSI_2 solutions in glymes containing Cl compared to Cl-free solutions.
- 2) **SEI formation**; Cl-based layers accumulate across the electrode-electrolyte interphase, forming SEI-like layer. This layer transports well Mg ions, but has poor electron conductivity, thus inhibiting the formation of irreversible passivation film or corrosion. Preliminary EQCM measurements in a variety of similar solutions indicated very large mass accumulation on inert electrodes (Au, Pt), that did not lead to electrochemical passivation. It was not possible, though, to tell mass accumulation from pronounced viscoelastic changes.
- 3) **Lowering desolvation/deligation energy**; Cl-free and Cl-containing solutions contain different electroactive species. The electroactive species in Cl-free $\text{MgTFSI}_2/\text{DME}$ is the solvate $3\text{DME}:\text{Mg}^{2+}$, while in ICD it is $[\text{5DME}\cdot\text{Mg}_3\text{Cl}_4]^{2+}$. It had already been established that the solvate constitutes very strong ligands (DME)-Mg bonds forming more stable species than in the complex $[\text{5DME}\cdot\text{Mg}_3\text{Cl}_4]^{2+}$ [11]. That is to say, freeing Mg ion (for Mg intercalation) from MgTFSI_2 in DME solutions is more energy intensive than in ICD. Hence, the third hypothesis postulates that Cl species lower the energy penalty for Mg deligation/desolvation. In the case of MgTFSI_2 solutions in DME addition of chlorides promotes the formation of Mg-Cl-DME complex ions, from which Mg ions are more liable for intercalation. Under this model the Cl ions plays important role in the charge transfer across the electrode/electrolyte interphase during intercalation, by reducing the energy required to strip the inserted ion from its solvation shell.

All the above three hypotheses were disproved by two simple experiments. First, CP electrodes were cycled in $\text{MgTFSI}_2/\text{DME}$, removed and subsequently cycled in ICD. Once put in ICD, the formerly inactive electrodes showed normal Mg intercalation behavior. Hence, cycling CP in $\text{MgTFSI}_2/\text{DME}$ solution does not affect the CP electrode performances in solutions that does support intercalation. **This observation refutes option 2, passivation inhibition by Cl-based species. If this hypothesis was true, the alleged passivation layer formed in the first stage, in $\text{MgTFSI}_2/\text{DME}$ solution, would have blocked the CP electrode from electrochemical activity (It is still possible that Cl ions act as dissolution/repairing agent for an already formed passive layer).**

In the second experiment, CP electrodes were cycled (6-8 CV cycles) in ICD, removed and transferred to $\text{MgTFSI}_2/\text{DME}$ solution for cycling. Surprisingly, these electrodes showed nearly all of the "normal" intercalation activity features (**Figure 5.1b**). Actually, the electrochemical signature of the CP in $\text{MgTFSI}_2/\text{DME}$, after the treatment in ICD, resembles that for CP in ICD, in terms of peak potential and reversible specific capacity (70-80 mAh/g). However, the CP showed sharper redox peaks in the ICD electrolyte solution, as well as smaller peaks separation. This suggests that the insertion process is still kinetically favorable in ICD compared to the Cl-free solution, even after treatment in ICD. **It is important to note that the pretreated CP electrodes in ICD had lasting effect on the electrochemical activity once transferred to the Cl-free solution, the solution that contains only the stable $3\text{DME}:\text{Mg}^{+2}$ solvate as the electroactive species. This result rebuts the option that Cl ions acts as surface dissolution/repairing agent or enable the intercalation process by reducing the desolvation energy for the Mg ions.**

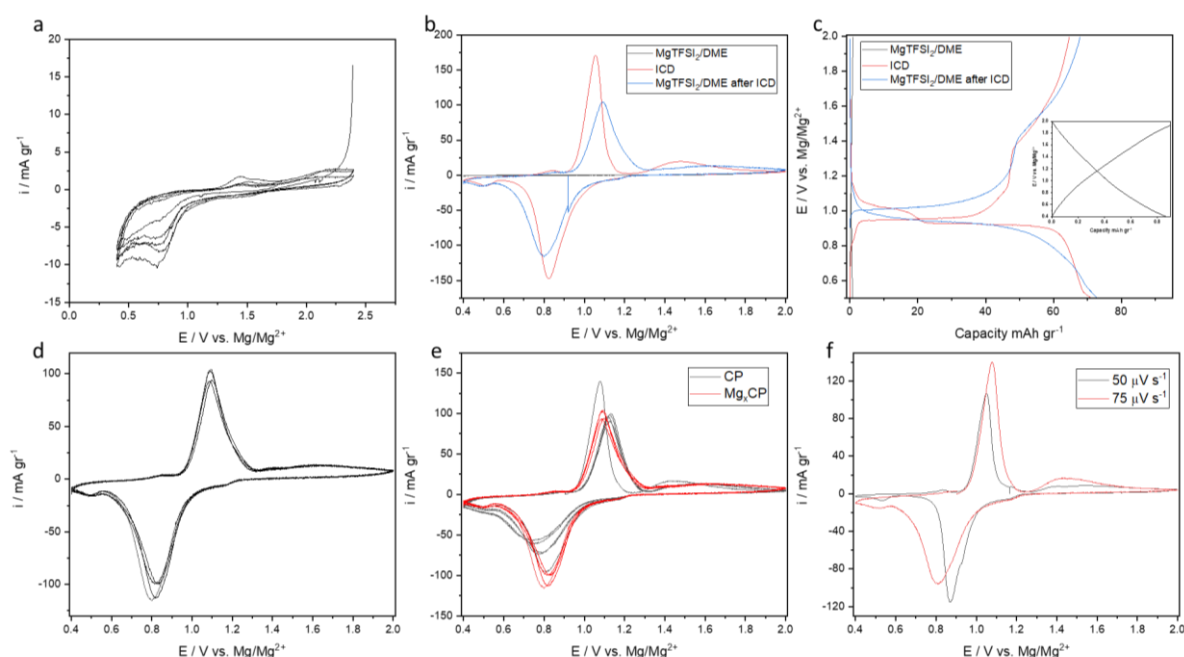


Figure 5.1: (a) Five first CV curves of CP electrode in Cl-free MgTFSI₂/DME, (b) Comparative steady state CV for CP electrode in Cl-free MgTFSI₂/DME (black), ICD (red), and Cl-free MgTFSI₂/DME after 8 CV cycles in ICD (blue), (c) Comparative chronopotentiometric curves of CP electrodes at C/10 in Cl-free MgTFSI₂/DME (black), ICD (red), and Cl-free MgTFSI₂/DME after 8 CV cycles in ICD (blue). Inset: steady state chronopotentiometric curves for a fresh CP electrode in Cl-free MgTFSI₂/DME, (d) First 4 CV cycles of CP electrode in Cl-free MgTFSI₂/DME after 8 CV cycles in ICD, (e) Comparative CV curves for Mg_xCP (black) and Mo₆S₈ (red) in Cl-free MgTFSI₂/DME after 8 CV cycles in ICD solution (Mg_xCP was obtained by a final LSV step to 0.4 V vs Mg after 7 CV full cycles). (f) The first CV cycle for pretreated Mg_xMo₆S₈ in Cl-free MgTFSI₂/DME at 50 and 75 μV/s after 8 CV cycles and final LSV to 0.4V vs Mg/Mg²⁺ in ICD. All CV's measurements were performed at a scan rate of 75 μV/s unless otherwise stated.

In addition, the pretreated CP electrodes showed stable CV and chronopotentiometric signatures with reversible specific capacity of around 70 mAh/g for at least 4 CV cycles (**Figure 5.1d** and **5.1c**).

In order to examine by which mechanism the pretreatment in ICD enables reversible intercalation process from Cl-free MgTFSI₂/DME, and what is the chlorides role in this process, it carried out two sets of experiments. In both treatments, CP electrodes were pretreated electrochemically in ICD by CV/galvanostatic charge-discharge cycling for full 8 cycles. The difference was the intercalation state of the electrodes upon pretreatment termination. Half were taken out at fully discharged state and the other half at fully charged one (*i.e.* Mg_xCP and CP, correspondingly). In the second part of the experiments the electrodes were carefully removed from the ICD solution, and put in Cl-free MgTFSI₂/DME for cycling.

As can be observed in **Figure 5.1e**, except for the first half cycle, the oxidation peak (de-intercalation process) has been independent on the pretreatment end-conditions. The intercalation peaks, however, has been much sharper with the electrodes that were Mg intercalated, Mg_xCP, at the termination of the pretreatment phase. These results indicate that the intercalation kinetics is dependent on the electrodes state at the pretreatment termination. When the pretreatment stopped with an intercalated CP, subsequent cycling in Cl-free solution shows better kinetics for intercalation and unchanged de-intercalation kinetics.

At first sight, this observation does not seem important. Yet, meticulous analysis of the implications of these results is of critical importance for the understanding of the chlorides effect on the electrochemical processes. The bulk, solid-state processes, occurring within the CP crystal during intercalation and de-intercalation are well understood; however, the interfacial processes taking place concurrently are less known, and seemingly are the key issue in this case. When the electrode is biased to negative potential (*vs.* OCV or PZC), positive ions in the



solution phase are attracted and absorbed onto the electrode's surface. In ICD the $[5\text{DME}\cdot\text{Mg}_3\text{Cl}_4]^{2+}$ positive ions contain chlorides.

Interestingly, and not less important, it also found out that even mere immersion the CP electrodes (at OCV) in ICD, without any electrochemical treatment, has nearly the same effect as electrochemical cycling. Meaning, simple chemical pretreatment with the Cl containing electrolyte solution, namely, ICD is sufficient to promote reversible intercalation process from the Cl-free solution. There still was a difference between the pretreatments regimes. The chemical pretreatment led to kinetically slower intercalation process in comparison with the electrochemically pretreated CP electrodes. The slower intercalation kinetics is expressed by substantially broader redox peaks, under the same electrochemical experimental conditions. These results may be very important also from applicative point of view, as chemical activation of electrodes, by simply soaking the electrode for a period of time in Cl-containing solution, is by far less demanding, and can be easily scaled-up. It did not run optimization experiments on this topic, but there is substantial evidence to suggest that such pretreatment can be accomplished very rapidly, in a matter of minutes rather than 48 hours.

From mechanistic and scientific point of view, this observation disproves the prospect that the activation process requires accumulation of charge and/or Mg ions inside the CP electrode.

Up to this point, the results show that at RT:

1. the intercalation process from Cl-free solutions is extremely poor or even null;
2. Electrochemical and chemical pretreatment in ICD promotes the intercalation process from Cl-free electrolyte solution, and
3. Electrochemical pretreatment that ends with discharged, Mg-containing CP improves especially the intercalation kinetics.

As mentioned above, intercalation processes entail sequential and concomitant steps. These include, among others, charge transfer across the solution/electrode interface (ions), charge transfer between the current collector (and the conducting additive)-intercalation material (electrons), ionic solid-state diffusion within the host, and accumulation. Each step is by itself complicated and may involve numerous, intricate processes. For example, the charge transfer across the solution/electrode interface may involve several sub-processes, such de-solvation, de-ligation and diffusion across SEI. The observations above clearly indicate that pretreatment of the CP electrodes in Cl-containing solution has decisive effect on the interfacial charge transfer process across the solution/electrode interface, rather than on the internal, solid-state diffusion or accumulation processes. However, the precise role of the chlorides, and the very identity of the interfacial species, is still unresolved.

Based on these unambiguous observations, and based on the following relations, **it formulates new hypothesis concerning the function of chlorides as Mg intercalation promoters. It hypothesizes that Cl-based ions (e.g. $\text{DME}\cdot\text{Mg}_x\text{Cl}_y$ complexes) bound to the CP surface and reduce the activation energy for Mg ions transfer across the electrode/solution interface. The simple expression below ties the kinetics of the charge transfer step to the activation energy during the course of the process**

$$k \propto e^{\frac{-\Delta G^*}{RT}} \quad (\text{Eq. 7})$$

Where k is the rate constant, G^* is activation energy, R is gas constant, and T is the temperature.

To expand the scope of the work, the same set of experiments were performed with a different solvent, AN instead of DME. Using AN as a solvent has several rationales:

- 1) The solvate $6\text{AN}\cdot\text{Mg}^{2+}$ is much less stable than $3\text{DME}\cdot\text{Mg}^{2+}$. Thus, the de-solvation effect can be relaxed[12].
- 2) The anodic stability of AN is much higher than the normal operation potentials of CP. Hence, surface passivation due to solvent oxidation and decomposition is less probable.
- 3) As much as it knows, AN does not stabilize complex ions' like $[5\text{DME}\cdot\text{Mg}_3\text{Cl}_4]^{2+}$. Thus, it can possibly get specific responses that may hints on the identity of the surface absorbed chlorides (complex or free Cl).



The electrochemical activity of CP electrodes in $\text{MgTFSI}_2/\text{AN}$ electrolyte solution also found to be very poor (**Figure 5.2a**). These findings are not unexpected because previous studies already showed that CP's electrochemical activity is relatively poor in AN based electrolyte solutions at room temperature[13]. At the first cycle, sharp reduction peak appears at -1.15 V vs. AC (*ca.* 0.9 V vs. Mg). This peak is assumed to correspond to Mg intercalation, although the charge associated is only *ca.* 30 mAh/g. This process is completely irreversible (kinetically and chemically) and during the next cycles this peak is completely absent.

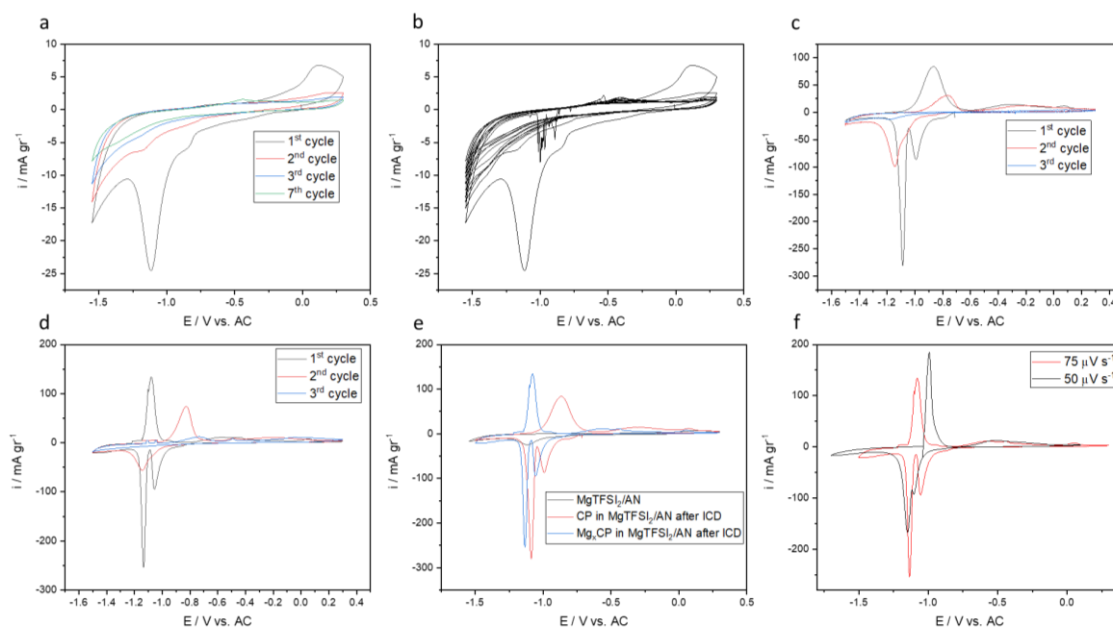


Figure 5.2: (a) CV cycles 1,2,3,7 of CP electrode in $\text{MgTFSI}_2/\text{AN}$, (b) 15 consecutive CV cycles in $\text{MgTFSI}_2/\text{AN}$, (c) The first 3 CV cycles of CP electrode in $\text{MgTFSI}_2/\text{AN}$ after 8 CV cycles in ICD, (d) The first 3 CV cycles of Mg_xCP in $\text{MgTFSI}_2/\text{AN}$ after 8 CV cycles in ICD, (e) Comparative CV curves of Mg_xCP (blue) and Mo_6S_8 (red) in $\text{MgTFSI}_2/\text{AN}$ after 8 CV cycles in ICD, (f) The first CV cycle of pretreated Mg_xCP in $\text{MgTFSI}_2/\text{AN}$ at 50 and 75 $\mu\text{V/s}$ after 8 CV cycles in ICD. All CV measurements were performed at scan rate of 75 $\mu\text{V/s}$ unless otherwise indicated.

This observation supports the refutation of the hypothesis that the Cl role in the intercalation process is to simply reduce the energy required for Mg desolvation/deligation. As noted before, $6\text{AN}\cdot\text{Mg}^{2+}$ solvation shell is markedly less stable than that with the trio-DME solvate.

Interestingly, after pretreatment in ICD, the same trend, as with Cl-free $\text{MgTFSI}_2/\text{DME}$ is obtained. After 6-8 cycles in ICD, the pretreated CP electrodes reversibly inserts Mg ions, with impressive kinetic cues, from the Cl-free $\text{MgTFSI}_2/\text{AN}$. However, in this case, the effect lasts one cycle only.

These experiments go in-line with the hypothesis that chlorides (probably Cl-containing complexes), adsorbed to the CP surface, act as game-changers. It suggests that the effects observed are due to specifically facilitated charge transfer kinetics across the solution/electrode interphase. The hypothesis is that strongly adsorbed chloride-based species reduce the activation energy for the specific stage of Mg-ion transport from the solution phase to the intercalation host. The results also reflect on the stability of the adsorbed species in the different solvents. Apparently, the adsorbed species are much more stable in ethereal solvent, like DME, compared with acetonitrile.

Figure 5.2c presents CV curves for CP in pure $\text{MgTFSI}_2/\text{AN}$ after 8 CV cycles in ICD pretreatment (ended at the de-intercalated state). In the first cycle, a very well defined and sharp reduction peaks are observed at 0.9 and 1 V vs. Mg, corresponding to Mg ions intercalation. However, at the back scan, the CV exhibits broad, sluggish re-oxidation peak. During the first full cycle, a reversible charge of 95 mAh/g passed. On the second cycle it already decreased to around 50 mAh/g, and later, in the third cycle, the electrode was completely inactive.



Figure 5.2d presents CV curves for CP electrode in MgTFSI₂/AN. Here again, the electrode was pretreated by cycling in ICD, but ended with intercalated CP, Mg_xCP. Interestingly, in a similar manner to cycling pretreated electrodes in Cl-free MgTFSI₂-DME, here also, when the activation ended with intercalated CP, the CV curve exhibited substantially sharp and well resolved oxidation peaks. This behavior indicates, again, that the final state of the activated CP (*i.e.* magnesiated or de-magnesiated CP) has a great impact on the de-intercalation kinetics in the Cl-free solution. It doesn't affect, though, the consecutive cycling stability.

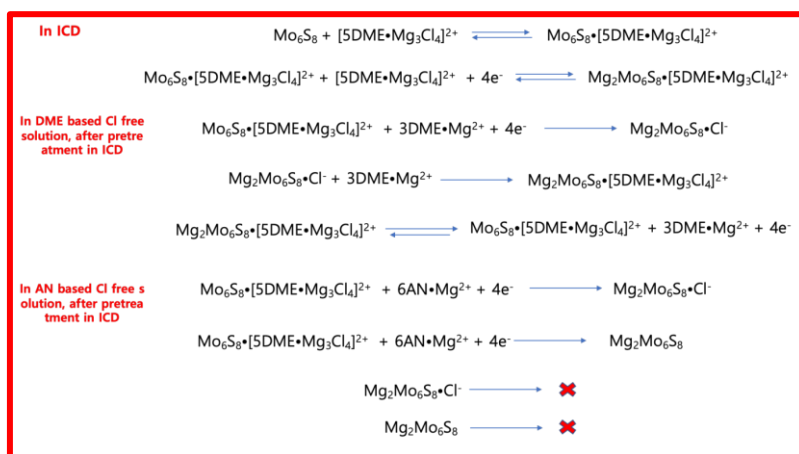
To sum it up, anytime that the pretreatment ends with Mg_xCP, the CV curves exhibit sharp reduction and oxidation peaks in the first cycle in the Cl-free electrolyte solution. On the other hand, when the pretreatment ends with charged CP (contains no Mg), the first CVs curves exhibit a sharp reduction peak, but a subsequent sluggish oxidation peak. These facts carry incidental information regarding the adsorbed species identity, in addition to the fundamental role of the chlorides in the intercalation mechanism.

The results strongly suggest that the adsorbed Cl-based species desorbs and removed from the CP surface when the electrode is biased to low potentials in AN based solution. In such a case, this entails that during discharge the adsorbed complex becomes negatively charged. The adsorbed complex from ICD, as mentioned above, is most probably the ubiquitous electrochemical active species, [5DME•Mg₃Cl₄]²⁺.

Based on these considerations, it proposes that:

- 1) **It is the complex cation [5DME•Mg₃Cl₄]²⁺ that primarily adsorbed onto the CP surface from ICD during the pretreatment.** Later on, during the first discharge in a Cl-free solution, Mg ion leaves the complex to be intercalated in the host, leaving free Cl⁻ anions (and, possibly, smaller fragments of the complex cation). The fate of the free Cl⁻ anions and the fragmented complex cations are very strongly dependent on the solvent.
- 2) **A pretreated electrode is active only for one cycle in AN based solution due to the adsorbed complex instability under specific conditions.** Under low voltage biasing and Mg removal, the [5DME•Mg₃Cl₄]²⁺ complex collapses and its constituents dissolve into the solution. In DME-based solution, the pretreated electrode, with its adsorbed layers, can be cycled many times, because the complex is maintained through the reservoir of Mg ions and DME molecules in the solution. In other word: during discharge of a pretreated CP electrode in MgTFSI₂/DME, Mg ions leave the [5DME•Mg₃Cl₄]²⁺ complex to enter the host, but complex-ion structure concurrently repaired with Mg ions and DME molecules from the solution. Thus after (or during) each Mg⁺² insertion, the intermediate Mo₆S₈•Cl⁻ restructures to the previous state, Mo₆S₈•[5DME•Mg₃Cl₄]²⁺ and the activation layer does not collapse and desorb. Obviously, such mechanism is unlikely to occur in AN-based solution, as it does not support the formation of similar, Cl-based, complexes.

The suggested Mg²⁺ intercalation mechanism and the chlorides (denoted as "Cl"), role in this process is illustrated in **Scheme 5.1**:



Scheme 5.1: Suggested intercalation mechanism of Mg ions into pretreated Chevrel phase and the role of "Cl" in the insertion process in DME and AN based solutions.



In order to challenge the above hypothesis, CP electrodes were pretreated in APC, in which the electroactive species is also a Cl^- based complex, though of different structure, $[\text{6THF}\cdot\text{Mg}_2\text{Cl}_3]^+$. As before, the treated electrodes were transferred to Cl-free $\text{MgTFSI}_2/\text{DME}$. In such case it was expected to obtain different CV signature, at least due to the solvent ligands exchange. However, if the specific identity of the adsorbed surface activation species is not critical, it would expect to observe similar trends in the CV characteristics as with the ICD pretreated electrodes.

Figure 5.3 presents the CV curves of CP electrodes in Cl-free $\text{MgTFSI}_2/\text{DME}$ after 8 cycles in APC.

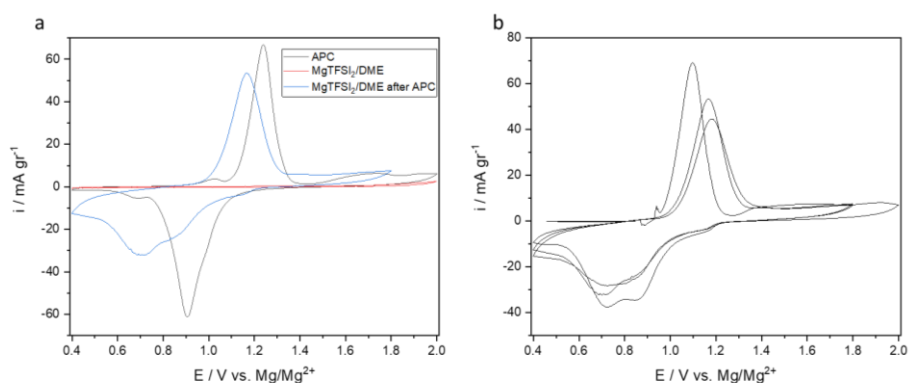


Figure 5.3: (a) Comparative steady state CV of CP electrode in $\text{MgTFSI}_2/\text{DME}$ (red), APC (black), and $\text{MgTFSI}_2/\text{DME}$ after 8 CV cycles in APC (blue), (b) The first 3 CV cycles of CP electrode in Cl-free $\text{MgTFSI}_2/\text{DME}$ after 8 CV cycles in APC. All CV measurements were conducted at a scan rate of $50 \mu\text{V/s}$.

The results clearly demonstrate that pretreatment in APC also promotes the reversible intercalation process of Mg ions from chloride free $\text{MgTFSI}_2/\text{DME}$. However, as expected, the electrochemical characteristics are somewhat different. The reduction peak is significantly wider, indicating, most probably, slower intercalation kinetics. This might be due to ligands exchange or the change in the nature of the activating surface complex.

These results strongly support the hypothesis that adsorbed “chlorides” are part of a complex structure rather than a free chloride.

Based on all the above results, it asserts that various specific, Cl-based electroactive complex species adsorb on the CP surface act as promoters for the charge transfer across the solution/host interface. In addition, intercalation promoting species remain strongly adsorbed for prolonged cycling periods only in electrolyte solutions containing (ethereal) solvents that can preserve the basic structure of the complexes.

Ex-situ XRD measurements of discharged CP electrodes (2 CV cycles and LSV to 0.4V vs. Mg/Mg^{2+} at a scan rate of $50 \mu\text{V/s}$) corroborated the poor electrochemical activity of CP in Cl-free electrolyte solutions. The influence of the electrolyte solution, or to be more specific, the chlorides presence, on the CP's intercalation activity can be obtained from the XRD patterns, as depicted in **Figure 5.4**. The major structural changes obtained in ICD reflect Mg intercalation to the expected levels based on the Faradaic charge. In the Cl-free solutions, the CP electrodes show hardly any change after attempted discharge in AN based solution. Surprisingly, attempted discharge in Cl-free $\text{MgTFSI}_2/\text{DME}$ show intermediate results.

To get better quantitative figures and to correlate the structural changes with the electrochemical results, Rietveld refinement has been done. It is important to note that some spontaneous chemical de-intercalation may occur when measuring intercalated samples under ambient conditions (reaction with water vapors and oxygen). This is especially true for the less stable, highly intercalated $\text{Mg}_2\text{Mo}_6\text{S}_8$ phase. $\text{Mg}_x\text{Mo}_6\text{S}_8$ ($x < 1$) is considered to be more stable.

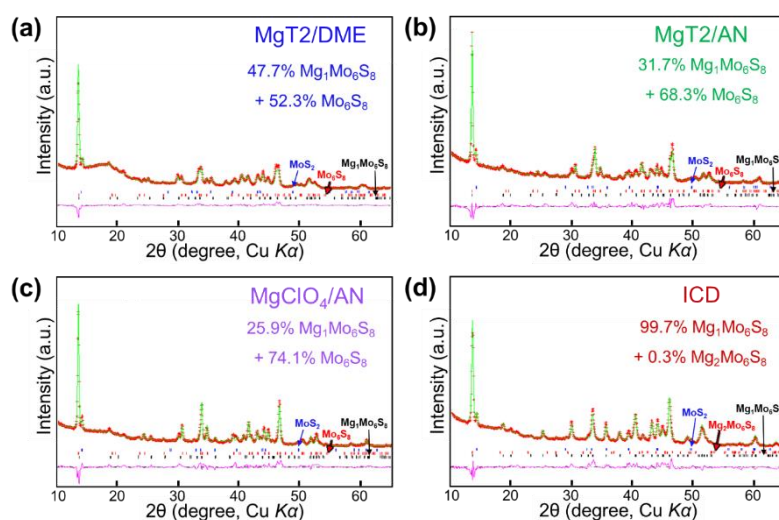


Figure 5.4: Rietveld refinement of the XRD patterns of discharged CP electrode in (a) MgTfSI₂/DME, (b) MgTfSI₂/AN, (c) Mg(ClO₄)₂/AN, and (d) ICD electrolyte solutions.

During the electrochemical process of CP in Cl-free MgTfSI₂/DME solution, a total charge of around 30 mAh/g passed (including the irreversible charge during the 2 CV cycles). This amount of charge is in a good agreement with the Rietveld refinement, which indicated that the CP electrode contains 47.7% of Mg₁Mo₆S₆ (corresponding to 28 mAh/g). In contrast, CP after discharge in ICD delivered a specific capacity of around 80 mAh/g, while the Rietveld refinement indicated that only 1 Mg ions per unit cell, corresponding to 62 mAh/g. However, as mentioned above, this highly likely due to chemical de-intercalation under exposure to atmospheric environment. With MgTfSI₂/AN, an accumulated charge of around 40 mAh/g passed during the electrochemical process. The Rietveld refinement indicated only 21 mAh/g worth of Mg in the host.

Electrochemistry is a very powerful analytical tool. It is sensitive, accurate and specific. Quite frequently it proves to be more sensitive and precise than many spectroscopic means. Nevertheless, surface analysis by XPS, despite its limitations, is indispensable in studying the chemical interfacial aspects of the hypothesis. For the XPS study we used binder and conductive additive free CP electrodes pressed onto stainless steel mesh current collectors. In such configuration we can learn about the CP electrode-electrolyte solution interaction with high precision, with the least interference from the inert components. Hereafter it presents only the most significant results, those that strong conclusions could be drawn from.

Figure 5.5 show the C 1s spectra acquired from several additives-free CP electrodes: a pristine CP electrode (5.5a), CP electrodes after: 5 CV cycles in ICD (5.5c); cycled in Cl-free MgTfSI₂/DME (5.5b) and an ICD pretreated CP electrode after 3 CV cycles in Cl-free MgTfSI₂/DME (5.5d). Except for the pristine electrode, all the electrodes show a clear peak at a binding energy of 293.1 eV. This peak corresponds to TfSI's CF₃. All electrodes contain peaks at binding energies of 288.9 eV, 286.6 eV and 285 eV, corresponding to carboxylates and carbon bound to one oxygen atom or ethereal solvent, and carbon bound to carbon or hydrogen, respectively[14,15].

These results indicate that no exclusive carbon-based surface passivation films develop on the CP electrodes in the different solutions. In fact, it shows that probably the same carbon-based surface chemistry develops on the CP electrodes, regardless the electrolyte solution nature. In another words, these results prove that the Cl role in the intercalation process is not related to preventing or stripping passivation films originating from electrolyte solution decomposition. In addition, we examined also the surface chemistry of CP electrodes that were only immersed in ICD for 48 hours. In this, also, the C 1s spectra show the same carbon-based surface composition.

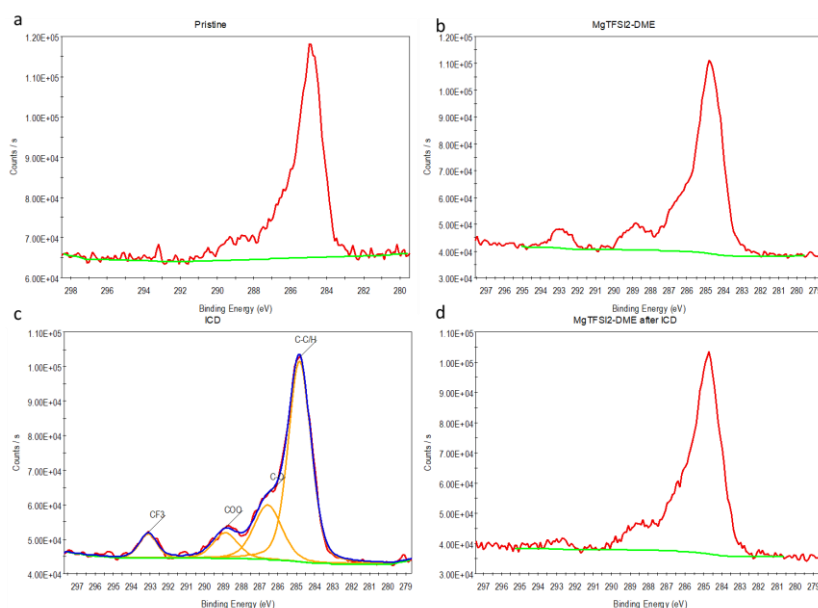


Figure 5.5: C 1s spectra of (a) pristine CP electrode, CP electrodes after 5 CV cycles in: (b) Cl-free MgTFSI₂/DME, (c) ICD, and (d) ICD pretreated electrode after 3 CV cycles in Cl-free MgTFSI₂/DME.

Figure 5.6 shows the Mo 3p spectra for the same set of samples. The Mo3p spectral region was selected since it is devoid of interferences from S 2p peaks and strong loss features. As shown in Figure 5.6 (Mo 3p spectra for immersed CP electrode in ICD) the Mo 3p_{3/2} spectra of all samples are of almost identical intensity. Obviously, peaks strength across samples can be meaningful only if it compares well with relative intensities of other element's peaks and background level. This is practically the case when taking into account the most important peaks heights, for C 1s, S 2p, O 1s and Mo 3d. This result also strongly suggests that the Cl role is not related to preventing or stripping passivation films.

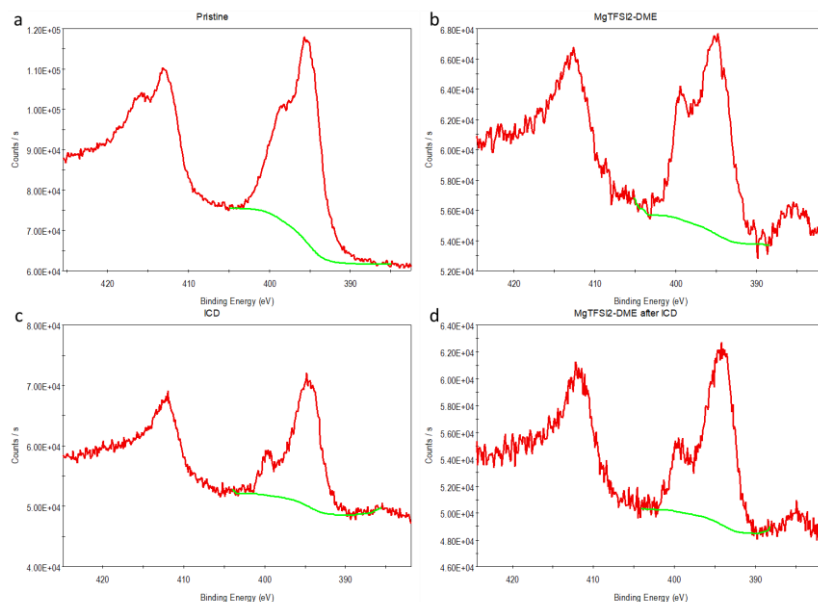


Figure 5.6: Mo 3p spectra for (a) pristine CP electrode, CP electrodes after 5 CV cycles: in (b) Cl-free MgTFSI₂/DME, (c) ICD, and (d) ICD pretreated CP electrode cycled in Cl-free MgTFSI₂/DME.



There are noticeable differences in the Mo 3p spectra for the different samples. The main difference is in the heights ratio for the peaks at around 395.3 eV (Hi) and 394.6 eV (Lo) eV. In a simplistic manner, it associates these differences to different Mg intercalation levels in the host, reflecting different Mo electronic density. The peak at the lower BE is associated with Mo at lower oxidation state, while the one at a higher BE is associated with Mo in a higher oxidation state. The spectra show that for the pristine and the Cl-free solution cycled samples, the Hi:Lo peaks ratios are larger than for the two others. This suggests that the two later ones indeed contain more structural Mg.

Unfortunately, the Mo 3d region is packed with too many features, associated with Mo and S, and complicated by spin-orbit couplings, different oxidation states and loss function. Thus, it opted not to over-interpret these spectra.

The Cl 2p spectral region for the same set of samples is presented in **Figure 5.7** and the corresponding Mo 3p/ Cl 2p quantification in **Table 5.1**. Based on the BE, all Cl 2p peaks corresponds to negatively charged Cl ion. Naturally, the pristine CP electrode shows no Cl-related features. The CP electrode cycled in Cl-free MgTFSI₂/DME contains trace Cl that can be due to minute Cl contamination in the solution or from cross contamination in the glove-box. On the other hand, the CP electrodes cycled in ICD contains substantial amount of adsorbed Cl. Much more revealing is the strong Cl 2p spectra obtained from the ICD-pretreated CP electrode that was cycled in Cl-free MgTFSI₂/DME. Actually, the Mo:Cl ratio for this samples is only slightly smaller from one cycled in ICD only, and still larger than the one measured for the ICD immersed only.

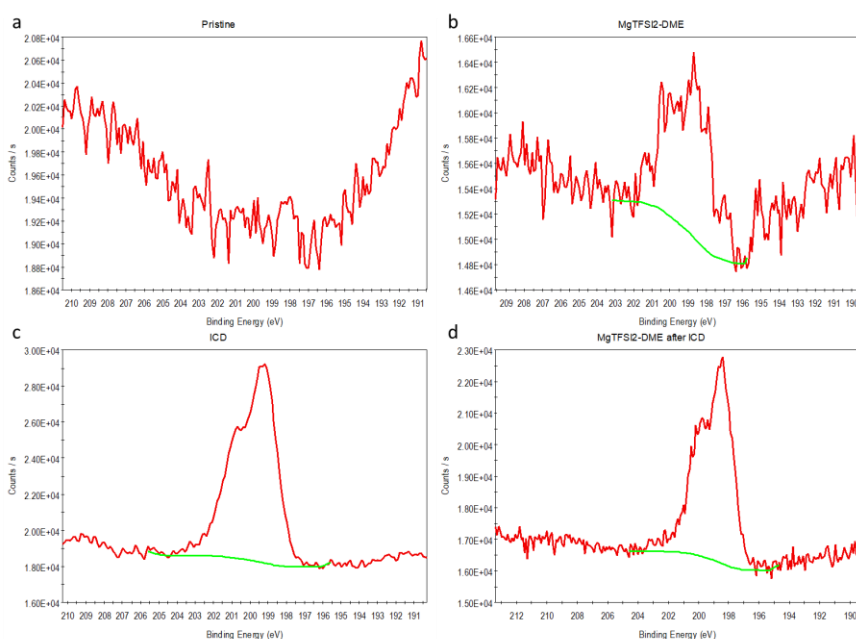


Figure 5.7: Cl 2p spectra for (a) pristine CP electrode; CP electrodes after 5 CV cycles in: (b) Cl-free MgTFSI₂/DME, (c) ICD, and (d) ICD pretreated electrode, subsequently cycled in Cl-free MgTFSI₂/DME.

Table 5.1: calculated Mo/Cl ratio on the surface of: pristine CP electrode, CP electrodes after 5 CV cycles in Cl-free MgTFSI₂/DME, CP electrodes after 5 CV cycles in ICD CP electrode immersed in ICD, and ICD pretreated CP electrode (5CV cycles in ICD) after 3 CV cycles in Cl-free MgTFSI₂/DME.

| | Pristine CP | Cycled in Cl-free MgTFSI ₂ /DME | Cycled in ICD | Immersed in ICD | Pretreated CP electrode cycled in MgTFSI ₂ /DME |
|-------|-------------|--|---------------|-----------------|--|
| Mo:Cl | 200:1 | 10:1 | 1.36:1 | 4.8:1 | 1.58:1 |



These results point to several important trends. The accumulation of adsorbed chlorides on the CP is both spontaneous and electrochemically driven. Quantitatively, the electrochemically driven chlorides buildup is significantly greater than the spontaneous one. The most intriguing result is that the chlorides concentration on the ICD treated CP is hardly affected by cycling in Cl-free solution. This result corresponds well to the electrochemical responses obtained in the different solutions.

Unfortunately, it is practically impossible to identify the exact nature of the chlorides in unequivocal manner. The BE for the Cl 2p corresponds to metal-Cl⁻ species. These can be Mg-Cl based complexes, as well as Mo-Cl ones, as suggested in some studies[16].

The XPS data for all samples exhibited also some common features. All electrodes (apart from the pristine) show F 1s at around 689 eV, corresponding to organic-based F, originating from the TFSI anions. The S 2p spectra for all electrodes but the pristine are very similar, with identifiable peaks at around 169.6 eV and 162.3 eV, corresponding to TFSI and sulfides, respectively. All the CP electrodes show O 1s peak at around 531.9 eV, probably related to adsorbed ethereal oxygen originating from DME molecules[14] and probably also due to some surface oxidized CP.

Although rich in data, due to its complexity, the surface analysis portrays limited, but important information. It clearly shows that except the for the Mo:Cl ratio and Cl and Mo oxidation states there are no substantial qualitative and quantitative differences in the surface chemistry of the CP electrodes despite their different histories.

5.1. Conclusions

The research described herein deals with a subject of critical importance related to the Cl role in the intercalation process of Mg ions into CP.

It may as well be of great importance for other, current and future cathode materials. **In addition, it presents here a new approach to activate CP cathodes for Mg batteries in Cl-free electrolyte solutions.**

Throughout this study it explored in depth the various possibilities by which chloride-based species affects the intercalation process of Mg ions into CP.

- It found out that at room temperature, CP, the only materials family known to truly reversibly host Mg ions with reasonable kinetics, possess poor electrochemical activity in "simple salts", Cl-free solutions.
- It also demonstrated that addition of "chlorides" to these electrolyte solutions, or pretreatment of the CP electrode in chlorides containing solutions, promotes reversible Mg intercalation with good kinetics also in Cl-free solutions.
- It suggests a comprehensive and detailed Mg ions intercalation mechanism scheme into CP that is consistent with all the experimental observations: The Cl⁻ ions, as part of a bigger complex, such as [5DME•Mg₃Cl₄]²⁺ adsorb onto the CP surface (*e.g.* in ICD). This strongly absorbed complex layer reduces the activation energy for the charge transfer reaction stage, in which Mg ions move across the solution/host interface. During intercalation, Mg ions and DME molecules leave the complex to form adsorbed CP-Cl⁻ intermediate species (Cl⁻ ion remains adsorbed). Shortly after, through reaction with the solution phase DME and Mg-based ions, the intermediate MoCl_x transforms back to the original adsorbate, *e.g.* [5DME•Mg₃Cl₄]²⁺. The adsorbed species were found to be exceptionally stable, enduring both electrochemical cycling in Cl-free solutions, and thorough washing and vacuuming for XPS analysis. Yet, the stability of these adsorbates is maintained only in electrolyte solutions containing solvent that is capable to stabilize its structure, at least to certain degree (*e.g.* DME or THF). In AN, for instance, the adsorbate rapidly collapses and washed away from the CP surface.



This study may open a hatch for future development in pairing cathode materials to magnesium anodes in Cl-free electrolyte solutions. In addition, it extends the know-how that may lead to utilization of novel cathode materials by judicious surface chlorination to facilitate Mg ions charge transfer across the solution/cathode interface.

6. Final highlights

1. It has determined quantitatively the influences of electrolyte solution into the kinetics and the thermodynamics of the intercalation process into the CP electrodes.
2. It is established that the formation of thin, passivating layer when V_2O_5 electrodes are cycled in TFSI-based solution cause serious impedance for Mg intercalation, and even a complete passivation.
3. The electrochemical behavior of V_2O_5 electrodes in the presence of DME, coupled with the solutions structure study, indicates that the intercalation process of Mg cations is affected strongly by the formation of stable solvation shell with DME. Hence, de-solvation of these DME based structures impedes very strongly the intercalation of naked Mg ions into the vanadium oxide host.
4. It should be noted that ethers in general and glyme solvents like DME in particular are very important for the field of Mg batteries since they allow reversible behavior of Mg anodes.
5. At room temperature, Chevrel phase, the only materials family known to truly reversibly host Mg ions with reasonable kinetics, possess poor electrochemical activity in "simple salts", Cl-free solutions. The addition of "chlorides" to these electrolyte solutions, or pre-treatment of the CP electrode in chlorides containing solutions, promotes reversible Mg intercalation with good kinetics also in Cl-free solutions.

7. Reference

- [1] E. Levi, YGofer, D. Aurbach, On the way to rechargeable Mg batteries: The challenge of new cathode materials, *Chem. Mater.* 22 (2010) 860–868. doi:10.1021/cm9016497.
- [2] R. Attias, M. Salama, B. Hirsch, R. Pant, Y. Gofer, D. Aurbach, Anion Effects on Cathode Electrochemical Activity in Rechargeable Magnesium Batteries: A Case Study of V_2O_5 , (2019) 6–11. doi:10.1021/acseenergylett.8b02140.
- [3] R. Attias, S. Bublil, M. Salama, Y. Goffer, D. Aurbach, Electrochimica Acta How solution chemistry affects the electrochemical behavior of cathodes for Mg batteries , a classical electroanalytical study, *Electrochim. Acta.* 334 (2020) 135614. doi:10.1016/j.electacta.2020.135614.
- [4] O. Chusid, Y. Gofer, H. Gizbar, Y. Vestfrid, E. Levi, D. Aurbach, I. Riech, Solid-State Rechargeable Magnesium Batteries, *Adv. Mater.* 15 (2003) 627–630. doi:10.1002/adma.200304415.
- [5] S. He, K. V Nielson, J. Luo, T.L. Liu, Recent advances on $MgCl_2$ based electrolytes for rechargeable Mg batteries, *Energy Storage Mater.* 8 (2017) 184–188. doi:10.1016/j.ensm.2016.12.001.
- [6] b N.P. and D.A. Robert E. Doe, Ruoban Han, a Jaehee Hwang, a Andrew J. Gmitter, a Ivgeni Shterenberg, b Hyun Deog Yoo, Novel, electrolyte solutions comprising fully inorganic salts with high anodic stability for rechargeable magnesium batteries, *Chem. Commun.* 50 (2014) 243–245. doi:10.1039/c3cc47896c.
- [7] J. Muldoon, C.B. Bucur, T. Gregory, Fervent Hype behind Magnesium Batteries : An Open Call to Synthetic Chemists — Electrolytes and Cathodes Needed *Angewandte*, (n.d.) 12064–12084. doi:10.1002/anie.201700673.
- [8] C. Liao, N. Sa, B. Key, A.K. Burrell, L. Cheng, L.A. Curtiss, J.T. Vaughey, J.-J. Woo, L. Hu, B. Pan, Z. Zhang, The unexpected discovery of the $Mg(HMDS)_2/MgCl_2$ complex as a magnesium electrolyte for rechargeable magnesium batteries, *J. Mater. Chem. A.* 3 (2015) 6082–6087. doi:10.1039/C5TA00118H.
- [9] R. Attias, M. Salama, B. Hirsch, Y. Goffer, D. Aurbach, Anode-Electrolyte Interfaces in Secondary Magnesium Batteries, *Joule.* 3 (2019) 27–52. doi:10.1016/j.joule.2018.10.028.
- [10] A.J. Bard, L.R. Faulkner, E. Swain, C. Robey, *Fundamentals and Applications*, n.d.
- [11] M. Salama, I. Shterenberg, L.J.W. Shimon, K. Keinan-Adamsky, M. Afri, Y. Gofer, D. Aurbach, Structural Analysis of Magnesium Chloride Complexes in Dimethoxyethane Solutions in the Context of Mg Batteries Research, *J. Phys. Chem. C.* 121 (2017) 24909–24918. doi:10.1021/acs.jpcc.7b05452.



- [12] R. Attias, M. Salama, B. Hirsch, Y. Gofer, D. Aurbach, Solvent Effects on the Reversible Intercalation of Magnesium-Ions into V₂O₅ Electrodes, *ChemElectroChem*. 5 (2018) 3514–3524. doi:10.1002/celec.201800932.
- [13] T.T. Tran, W.M. Lamanna, M.N. Obrovac, Evaluation of Mg[N(SO₂CF₃)₂]₂/Acetonitrile Electrolyte for Use in Mg-Ion Cells, *J. Electrochem. Soc.* 159 (2012) A2005–A2009. doi:10.1149/2.012301jes.
- [14] Y. Gofer, R. Turgeman, H. Cohen, D. Aurbach, XPS investigation of surface chemistry of magnesium electrodes in contact with organic solutions of organochloroaluminate complex salts, *Langmuir*. 19 (2003) 2344–2348. doi:10.1021/la026642c.
- [15] S. Leroy, F. Blanchard, R. Dedryvère, H. Martinez, B. Carré, D. Lemordant, D. Gonbeau, Surface film formation on a graphite electrode in Li-ion batteries: AFM and XPS study, *Surf. Interface Anal.* 37 (2005) 773–781. doi:10.1002/sia.2072.
- [16] L.F. Wan, B.R. Perdue, C.A. Ablett, D. Prendergast, Mg Desolvation and Intercalation Mechanism at the Mo₆S₈ Chevrel Phase Surface, *Chem. Mater.* 27 (2015) 5932–5940. doi:10.1021/acs.chemmater.5b01907.